STATISTICAL DOWNSCALING OF FUTURE RAINFALL AND TEMPERATURE UNDER DIFFERENT CANESM2-RCP MODEL SCENARIOS

By

FRANKLINE RONO

I45/7720/2017

DEPARTMENT OF METEOROLOGY

UNIVERSITY OF NAIROBI

P.O. BOX 30197-00100

NAIROBI, KENYA.

A research project submitted in partial fulfillment of the requirement for the award of **Postgraduate Diploma in Meteorology** of University of Nairobi.

NOVEMBER 2018

Declaration

I hereby declare that this dissertation is my original work and has never been presented for an award of a degree in any other university.

Signature …….. Date ……..

FRANKILNE RONO
Department of Meteorology
University of Nairobi
P.O Box 30197
Nairobi, Kenya

This dissertation has been submitted for examination with our approval s university supervisors;

Signature …….. Date ……..

PROF. JOSEPH M. ININDA
Department of Meteorology
University of Nairobi
P.O Box 30197
Nairobi, Kenya

Signature …….. Date ……..

DR. JOSEPH N. MUTEMI
Department of Meteorology
University of Nairobi
P.O Box 30197
Nairobi, Kenya

Acknowledgements

I acknowledge God for granting me sound health and his gift of long suffering and endurance.

Through the guidance and directions from Prof. Ininda and Dr. Mutemi, it was possible to make progress, beating deadlines and eventually meeting the objectives of the research study.

I extend my acknowledgement to the efforts and prayers from my wife, son and family members to ensure that I was constantly in good attitude.

I am most obliged to the Kenya Meteorological Department for granting me climate data that was used for the current study free of charge.

Abstract

The current study downscaled daily rainfall and temperature from Canadian Second Generation Earth Systems Model (CanESM2) in Uasin-Gishu County.

The main objective of the study was to determine the future daily rainfall and temperature characteristics projected form the Global Climate Model (GCM) under two representative concentration pathways (RCP 4.5 and RCP 8.5). Outputs from GCMs are of a coarser resolution and therefore require downscaling to local scales to allow for practical applications in specific areas of interest.

Methodology for the study involved: (1) estimation for the missing data; (2) analysis of the current climate characteristics; (3) screening of predictor variables; (4) statistical synthesis of climate from the statistical downscaling model (SDSM); and (5) analysis of the projected climate characteristics.

The results from the present climate show that both rainfall and temperature have been increasing over time since the year 1974 to 2017 with a change of 2.4 mm and 0.01^0C correspondingly. The future downscaled climate indicated a downward and an upward trend for temperature and rainfall respectively from the year 2006 to 2099 under both RC P4.5 and RCP 8.5. The model was quite skillful.

There was a substantial amount of missing data and recommend augmentation with the remote sensed climate from satellites in the future studies. The warming consistency over the study area points to a possible insurgence of malaria causing mosquitoes (highland malaria), which will be a threat to the health of people of Uasin-Gishu County and its neighbourhoods. Also due to increasing temperatures, there will probably be increased and alternating frequencies of above and below normal rainfall.

Since Eldoret town is experiencing rapid development, it implies that there is a corresponding increment in land area under concrete surface. What this means, in an event of above normal rainfall, is that there will be flooding. It is advised that the road, building and construction sectors

consider redesigning bridges, run-off pathways and related structures to accommodate for the coming flooding menace.

Table of Contents

List of figures

List of Tables

List of Acronyms

Acronym	Meaning
CanESM2	Canadian Second Generation Earth System Model
CGCM	Coupled Global Climate Model
CMOC	Ocean Carbon Model
CTEM	Terrestrial Carbon Model
ERF	Effective Radiative Forcing
GCM	Global Climate Models
GEP	Gene Expression Program Programming
GHG	Greenhouse gas
IPCC	Inter-governmental Panel on Climate Change
LARS-WG	Long Ashton Research Station Weather Generator
NCAR	National Center for Atmospheric Research
NCEP	National Center for Environmental Prediction
NCEP	National Center for Environmental Prediction
RCP	Representative Concentration Pathway
RF	Radiative Forcing
SDSM	Statistical Downscaling Model
SRES	Special Report on Emission Scenarios

CHAPTER ONE

1.0 Introduction

About 80 percent of one billion people living in Africa depend of crop and livestock farming practices as the source of their livelihoods (Sonwa et al., 2016). According to Sonwa et al. (2016), weather and climate variability and change is witnessed across Africa in different agro-ecological surroundings and populations are reacting to it.

Agriculture industry is the second biggest contributor to gross domestic product in Kenya. In Kenya, the sector provides for self-employment opportunities and accounts for the 60 percent and 16 percent of the foreign exchange and formal employment respectively (Muraya & Ruigu, 2017).

It is imperative that there is need for scientific knowledge about climate conditions that influence agricultural industry for sound decision making in times of climate change and global warming. With such improved understanding about Rainfall and temperature, it is possible to plan well for the agricultural production and hence improve on the crop and animal yields. This will go a long way into subduing food insecurity.

1.1 Statement of the Problem

Humans are multiplying very fast and responding to risks associated with climate change on earth (Sonwa et al., 2016). Climate change and climate variability have continued affecting the environment as well as the way human beings live. Therefore, there is an urgent need to take measures for adaptation and mitigation. In order to do this, there must be a source of scientific information to be used for making sound decisions by stakeholders concerned.

Proper, planned and systematic forecasting methods of the future Rainfall and temperature variability, which is the main indicator of climate change, ought to be developed down to the finer scales that are applicable for use at the local geographical scales. It is possible to detect the signals of global climate change from large-scales to station-level scales by use of downscaling techniques.

In order to understand climate change and climate variability, it is often common practice to use the Global Climate Models (GCMs) output datasets. The outputs from GCMs are seldom in a form that can be used directly to studies of the impacts of climate change on natural or human systems (Jones, Thornton, & Jens, 2009). GCM outputs are of coarse resolution, a property that limits its use for practical applications in the local scales.

In the twentieth century, clean water resources have kept dwindling as a result of the rapid growth in human population, poor water management practices and elevated levels of atmospheric pollutions as a result of human induced activities (Rwigi, Muthama, Opere, Opijah, & Gichuki, 2016) .

This proposal intends to quantify the future scenarios of Rainfall and temperature distribution in Kenya for effective climate change strategic decision making.

1.2 Overall objective

To determine the future daily rainfall and temperature characteristics projected from Global Climate Model under two Representative Concentration Pathways (RCPs) Scenario.

1.3 Specific Objectives

i To analyze the current climatic pattern using selected climate parameters
ii To downscale the projected climatology from RCPs using the SDSM
iii To validate the model
iv Determine the future characteristic rainfall and temperature from each RCP

1.4 Hypothesis

v There is no climate change signal in the present climate.
vi SDSM is capable of resolving the finer details
vii The model is capable of not reproducing the observed pattern
viii The future climate characteristics are the same as the present.

1.5 Justification

In the recent years, most parts of Kenya have encountered alternating extremes of droughts and above normal rainfall. There have been rampant cases of flooding which have caused deaths of humans and animals, in equal measure, as well as destruction to properties in Kenya in the resent times. Such climate variabilities have had direct influence on the agricultural production, which in turn has impacts on livelihoods and food security. With the rapid growing population, there is a corresponding increase in the associated risks to the drought and flooding events.

Generally, conclusions concerning impacts of risks related to climate change have conventionally been drawn from large-scale Global Climate Models (GCM), which often fail to capture the finer details about the regional and local levels. In order to predict climate conditions and the associated hazards, to enable planning in advance, there is need to source for information applicable to local scales. One way of doing this is to downscale the low-resolution GCM outputs to observation-station level scale.

Downscaled daily rainfall, temperature and other climate variables are applicable for use in: (1) impact assessment, (2) water resource modelling, (3) planning and management, (4) crop farming, (5) driving systems used for monitoring climate change impacts, (6) designing of hydro-meteorological structures and systems and (7) use in policy and decision making in the county levels of government.

From the available literature review there is hardly any detailed research that has been in Uasin-Ngishu County to downscale climate from GCMs. This project filled in the gap by using statistical downscaling of rainfall and temperature in Uasin-Gishu County.

1.6 Study area

The study area covers Uasin-Gishu County in Kenya. Uasin-Ngishu County borders Kericho, Nandi, Bungoma and Tranzoia counties to the South, South West, West and North respectively.

Uasin-Gishu has a cool and temperate weather conditions with two rainy seasons. The March-May (MAM)and December-January (DJF) are the wettest and driest seasons respectively. On average, the area receives an annual rainfall between 900mm and 1200mm and temperatures ranging from 8.4 ^{0}C to 27^{0}C.

Horticulture, dairy farming, large scale production of wheat and maize form the main economic activities. The county is also famous known as home of champions, owing to the high profile athletes training and living within the city of Eldoret. Uasin-Gishu county has a population of 894,179 (Census 2009) with half being persons of either gender. Most of the people in the county, about 289,380, live in Eldoret town which is the administrative headquarters of Uasin-Gishu.

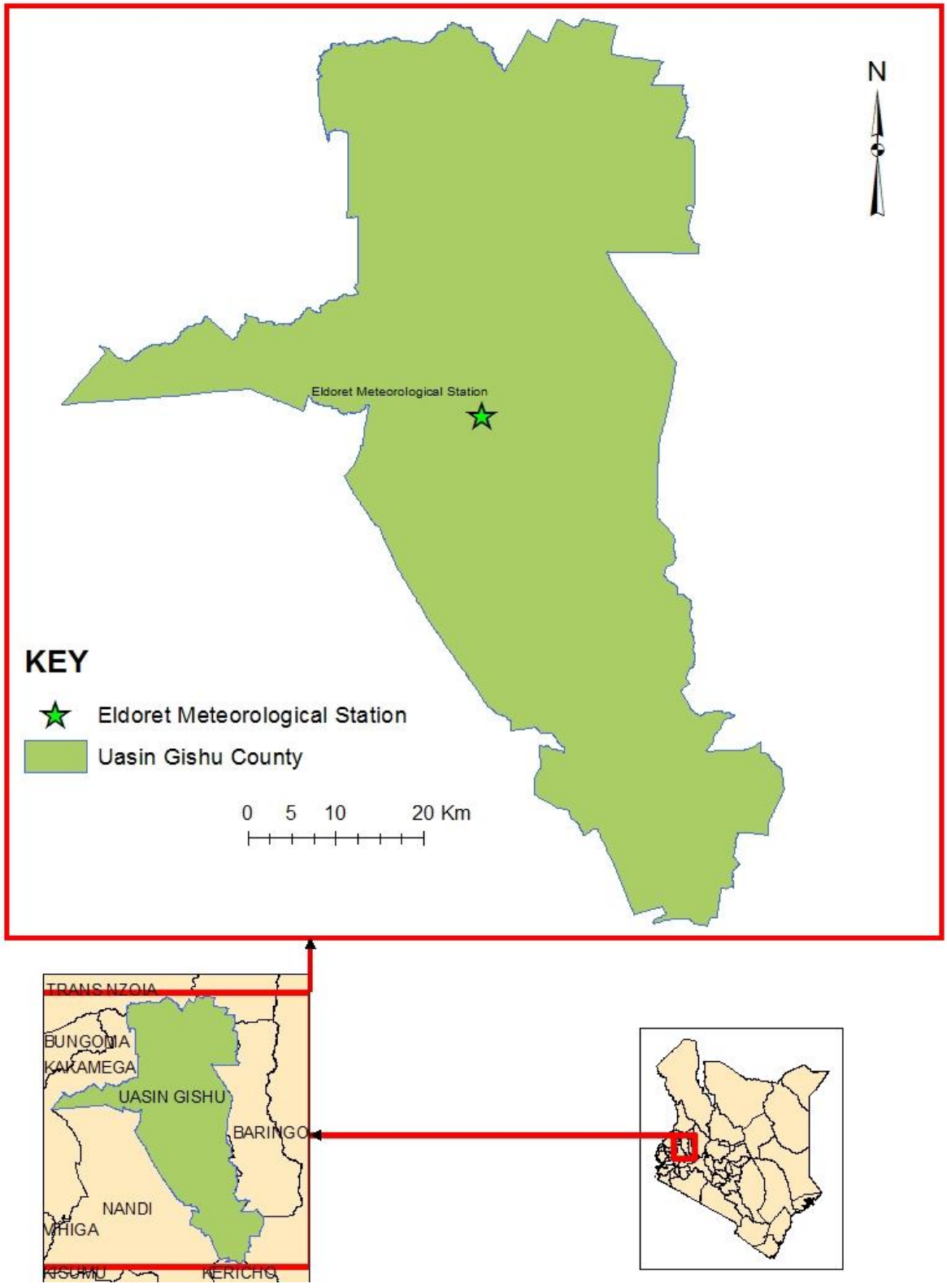

Figure 1: The study area-Uasin Gishu County

CHAPTER TWO

2.0 Literature Review

A number of researchers have carried out studies on development and evaluation of downscaling models, skill testing, and simulations of future climate scenarios. In their study, Mtongori et al. 2016 projected precipitation parameters such as total precipitation, wet-day frequency and wet-day mean using statistical downscaling methods over the republic of Tanzania. They found out that features of wetter and drier weather characteristics differ from station to station and season to season (Mtongori, Stordal, & Benestad, 2016).

Okkan and Kirdemir (2016) downscaled monthly rainfall statistically from CMIP5 datasets under RCP4.5, RCP6.0 and RCP8.5 over Gediz Basin in Turkey. Their methodology encompassed the ensemble of the GCM, Bayesian averaging and bias correction entailed Least-squares support vector machine (LSSVM) and artificial neural networks (ANN) procedures. Their findings were less significant decreasing trends of rainfall under RCP4.5 and RCP8.5 and more for RCP8.5 (Okkan & Kirdemir, 2016).

Keellings (2016) conducted a study comprising of mean and daily extreme maximum temperatures consist of downscaling of ensemble of the model outputs from CMIP5 in southeastern United States. The outcomes of the study demonstrated the ability of the model to significantly simulate the observed mean temperatures and pointed out to the limitation of downscaled models not being able to mimic the event of the extreme daily maximum temperature beyond 90 percent of the study area (Keellings, 2016).

Ininda et al. 2008 downscaled the Echam model outputs and used statistical modeling to forecast seasonal rainfall in Tanzania (Ininda, Athumani, & Mutemi, 2008). There are other several other studies applying statistical downscaling. Coupled Model Inter-comparison Project Phase Five (CMIP5)

According to Taylor et al. (2012), the origin of coupled model inter-comparison project phase five (CMIP5) dates back to September 2008. The working group on coupled modelling (WGCM) of the world climate research program (WCRP) agreed to come up with freely and readily available

multiple-model datasets. The goal of such multi-model outputs was to enhance understanding of the climate change and climate variability. The climate change CMIP5 experiment strategy involve long term (100 year) and near term (10 -30 year) integrations (Taylor, Stouffer, & Meehl, 2012).

2.1 Climate Change Signal

There are numerous studies that have been done to link climate change signals from Global Climate Model (GCMs) to the local scales in many parts of the world. Downscaled signals vary in extend and time with different representative concentration pathways (RCPs). Most of the studies done have shown consistent warming in different parts of the world including but not limited to Daksiya et al., (2017), Feyissa et al., (2018) and Tahir et al., (2018). Studies involving downscaling precipitation from GCMs indicate varying trends in annual and seasonal climate conditions as well as seasonal cycle shifts with different extends (Daksiya, Mandapaka, & Lo, 2017; Feyissa, Zeleke, Bewket, & Gebremariam, 2018; Mtongori et al., 2016; Tahir, Hashim, & Yusof, 2018).

A study was done by Tahir et al., (2018) in Lumbang River Basin, Sarawak, to examine the severity of the future rainfall under three different Representative Concentration Pathways (RCPs) in the period 2071 to 2100. Tahir et al., (2018) performed rainfall downscaling from the CanESM2 model outputs in three different RCPs for the period 2071 to 2100. The results under RCP 2.6, RCP 4.5 and RCP 8.5 indicated increase of rainfall by 8.13, 14.7 and 40.6 percent respectively. Over Lumbang River Basin, as was found out by Tahir et al., (2018) , there will most likely be a notable increase in the projected rainfall between 2071 and 2100 as compared to the baseline climate for the period 1976 to 2005, indicating the extend of climate change signal from the CanESM2 model.

In Addis Ababa city, Ethiopia, Feyissa et al., (2018) downscaled temperature and precipitation from two representative meteorological station. Their objective was to determine the change and extent of extremes in the climate variable from the climate change signals of Coupled Global Climate Model (CGCM3A2) and the Canadian Second Generation of the Earth System Model (CanESM2) models under RCP 4.5 and RCP 8.5 from the year 2020 to 2080. Results of their study

indicated increasing trends in both temperature and precipitation over Addis Ababa City under the two representative concentration pathways. From the findings Feyissa et al., (2018) indicated that the highest increases of minimum and maximum temperatures were found to be approximately 0.1 ^{0}C/decade and 0.3^{0}C/decade respectively under RCP 4.5 climate change scenarios (Feyissa et al., 2018). Also, extreme temperature indices were found to increase generally over the city. Rainfall was found to increase up to about 16.62 percent by 2080 under RCP 8.5.

In a study in Jakarta, Indonesia, was carried out by Daksiya et al., (2017) to quantify the impact of climate change on the frequencies of daily precipitation. As part of methodology, they used statistical downscaling model (SDSM) to downscale rainfall using CanESM2 model outputs to determine changes in the extreme events. Daksiya et al., (2017) found out upward trend in the wet seasonal and the annual precipitation characteristics of about 20 percent in a century cycle.

Mtongori et al., (2016) did a study to establish a link in the climate change signals in the Global Climate Models and the local scale climate characteristics in Tanzania using statitiscal downscaling methodology. They examined the total, wet-day mean and wet-day frequency charateristics of rainfall in three rainy seasons in Tanzania. Mtongori et al., (2016) study applied a multiple-model mean technique under RCP 4.5 and RCP 8.5 for the near-term, mid-century and end-century future time periods . the results indicated that OND rain. The mean of multiple-model simulations indicated a shift by October-December and December-April rainy seasons to wetter and drier conditions respectively.

Sonwa et al. (2016) conducted a study over African continent which found out how climate related risks have been responded to by the growing human population. They showed the how farming activities are executed and the effects of the climate variabilities. Agricultural practices are done in small scales in Africa and through direct rainfall. Increased frequency of climate variabilities, according to Sonwa et al. (2016), will alter the duration and success of growing seasons to crop production. The upward or downward trends of temperature or precipitation will affect the water resources. Since agriculture is dependent on the water balance component paramount in agriculture, implications on water resources have a corresponding influence on agriculture. Sonwa et al. (2016) found out that people in Africa have already responded to climate change by reducing

overdependence on farming and begun to diversify livelihoods by engaging in other income generating activities not directly linked to agriculture. Recommendation by Sonwa et al. (2016) points out that mitigation to climate change requires not only quick fixes like developing high productive and more adapted crops but to also study and obtain information about complex interrelationships among many factors that give rise to climate change risks.

2.2 Global Climate Models and the Future scenarios of climate change

Global Climate Models also known as the General Circulation Models (GCMs) are computer algorithms that implement equations of motions. Such computer programs (GCMs) compute approximate solutions to equations of motions in the form of Numerical Weather Prediction (NWP). GCMs are installed and run in specialized computers which then approximate numerical solutions grid by grid hence enabling predictions of weather patterns in space and time. Some of the examples of GCMs include CanESM2, GISS-E2-H, HadGEM2-AO, CCSMA4, and many others (Mtongori et al., 2016; Tahir et al., 2018).

2.3 Representative Concentration Pathways (RCPs)

Understanding about RCPs requires knowing about the greenhouse gases in the atmosphere whose greenhouse-effect has contributed the largest to the global warming. Such gases include methane, carbon dioxide, nitrous oxide, hydrofluorocarbons, Sulphur hexafluoride and perfluorocarbons (Meehl et al., 2007; Myhre et al., 2013).

Radiative forcing is the net change of the earth system's energy balance brought about by some external disturbance imposed to it (Myhre et al., 2013). Computed values of radiative forcing provide a means for comparing the responses of climate to different agents exposed to it, especially the average global temperatures. According to Myhre et al. (2013), the occurrence of climate change happens when the climate system of the earth's atmosphere responses by counteracting with any changes in induced to the existing energy fluxes. There are two often used measures relating to the quantification of radiative forcing that include the effective radiative forcing (ERF) and the radiative forcing (RF) (Meehl et al., 2007; Myhre et al., 2013).

RF refers to the net change in the downwelling radiation flux at the tropopause level after a length of time when the temperatures within the strotosphere stabilize to equilibrium of the radiation, whereas keeping the temperatures and variables of state such as water vapour on the surface and troposphere constant. ERF, on the other hand, refers to the net change in the downwelling radiation flux at the topmost level of the atmosphere after a length of time when the water vapour, clouds and temperatures in the atmosphere are left to readjust while holding the sea-ice cover and sea surface temperatures constant (Myhre et al., 2013).

In order to provide a basis from which climate modeling can be compared in the study of climate science, it has become inevitable to use climate scenarios (Wyne,2013). According to Wyne (2013) scenarios are necessary to standardize metrics, assumptions, baselines and starting points, validate a model from another independent, and to have a seamless communication among various climate modelers. A short history of the progress Intergovernmental Panel on Climate Change (IPCC) of the climate change scenarios outlined by Wayne (2013) is shown in table 1.

Table 1: Climate Change Scenarios Since the inception of IPCC in 1988

Scenario	Scenario code	Year established
First Assessment Report	FAR	1990
1992 IPCC Supplementary Report	IS92	1992
Second Assessment Report	SAR	1996
Special Report on Emissions Scenarios	SRES	2000
Third Assessment Report	TAR	2001
Fourth Assessment Report	AR4	2007
Fifth Assessment Report	AR5	2014

The current study is based on climate change scenarios found in the fifth Assessment Report (AR5) IPCC report. Each RCP has a different plausible future prediction and accumulated concentrations of greenhouse gas emissions (Wayne, 2013).

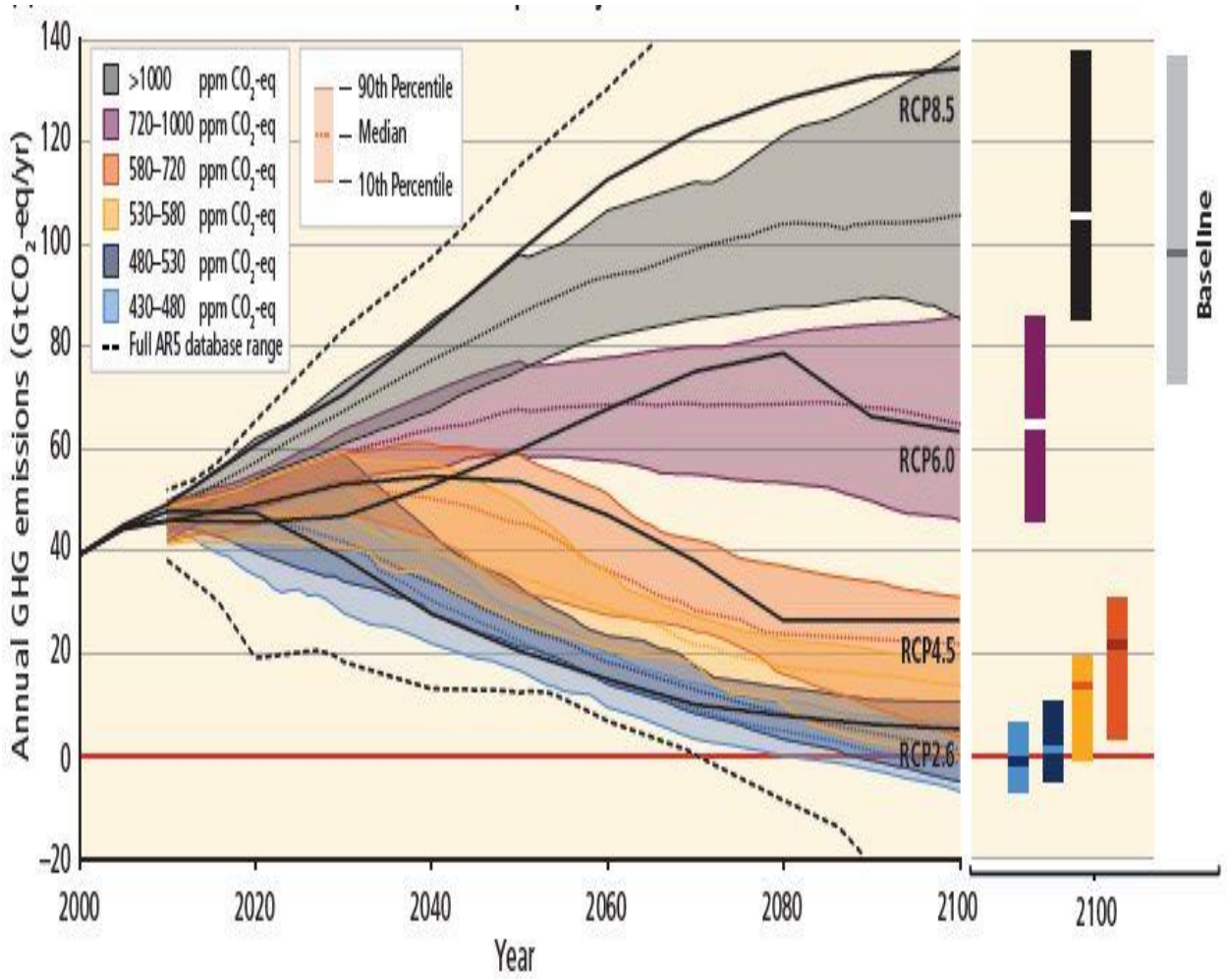

Figure 2: Emission pathways (trajectories) of greenhouse gases 2000-2100 : source (IPCC, 2014)

IPCC (2014) outlines four representative concentration pathways (RCPs) as shown in figure 1. To begin with, RCP 8.5 has a radiative forcing maintains an upward trend to approximately 8.5 watts per square meter by the year 2100 and keeps on increasing upwards. Secondly, RCP 4.5 and RCP 6.0 are the two intermediate RCPs that stabilize radiative forcing at 4.5 and 6.0 watts per square meter respectively by 2100. Thirdly, RCP 2.6 rises to its peak at about 3 watts per square meter way before 2100 and then maintains a downward trend.

For the RCP 4.5 and RCP 8.5 climate change scenarios used in the current study, the anthropogenic greenhouse gases (GHCs) concentrations have carbon-do The four RCP pathways represent carbon

equivalents (CO_2-eq) are 650 and 1370 parts per million (ppm) respectively (Mtongori et al., 2016; Okkan & Kirdemir, 2016).

RCP 4.5 is a long-term scenario that encompasses emissions of greenhouse gases, short-lifespan species, land use and land cover globally that is expected to level up without exceeding 4.5 watts per unit square meters (Wm^{-2}) by the year 2100 (Thomson et al., 2011). In terms of carbon dioxide equivalence scale, radiative forcing of 4.5 Wm^{-2} is approximately 650 parts per million (ppm) CO_2-equivalent. RCP 4.5 climate scenario relies on the supposition that policies, regulations and legislations, such as the carbon credit, will be put in place to help curb greenhouse gas emissions by setting limits that will result in the stabilization of the radiative forcing by 2100.

2.4 Importance of downscaling

Downscaling is a technique used to convert information known at large-scale areal coverage to predict phenomena at local scales. The two major techniques involved in climate downscaling are statistical and dynamical.

Statistical climate downscaling is a dual-step method which involves (1) development of empirical-statistical relationships between predictand (local climate variables) and the predictors (larger-scale climate variables), and (2) using such associations to simulate the future local climate behavior using outputs from the general circulation models (GCMs). Wilby et al., (2004) lists strengths, weaknesses and a number of statistical downscaling techniques including synoptic weather typing, transfer-function procedures, and stochastic weather generators.

According to Wilby (2002), weather typing consists of organizing of meteorological data at local scales with respect to prevailing atmospheric patterns. Examples include distributions of extreme values, and cluster analysis. Stochastic weather generation involves the modification of parameters belonging to the conventional weather generators such as conditional probability, and Markov-type techniques. Thirdly, transfer function method is dependent on the empirical-statistical relationships between the local-scale dependent variables (predictands) and the independent variables (predictors) at the regional scale (Wilby, 2002; Wilby & Dawson, 2004). This procedure

includes artificial neural networks (ANNS), regression, and canonical correlation analysis (Okkan & Kirdemir, 2016; Wilby, 2002).

Dynamical downscaling is the nesting of the Regional Climate Model (RCM), which is of a finer resolution, inside a lower resolution General Circulation Model (GCM). It necessitates the use of observed data or local-scale outputs from climate models, as boundary conditions, to run sub-regional domain finer resolution models. Some of the limitations associated with this procedure are: (1) it requires high-powered computers, and (2) it generates future scenarios that are dependent on the boundary conditions used to initiate simulations.

2.5 Canadian Second Generation Earth System Model (CanESM2)

Canadian second generation version of the earth systems model (CanESM2) is one of the global climate model established through a process in which the Coupled-Ocean-Atmosphere physical version of the Model (CanCM4) is coupled with two models namely: terrestrial-carbon model (CTEM) and the ocean-carbon model (CMOC) (Feyissa et al., 2018). CanESM2 is one among the many global climate models incorporated in the coupled model phase five inter-comparison project (CMIP5) which is adopted in accordance with the recommendation of the fifth report of the IPCC (Brekke, Thrasher, Maurer, & Pruitt, 2013).

CanESM2 model is made up of the atmosphere, sea ice, ocean and land realms together with the models of the carbon cycle (Yang & Saenko, 2012). According to Yang and Saenko (2012), the CanESM2 ocean component was adopted from the community model version of the ocean of the NCAR with 1.41^0 by 0.94^0 horizontal resolution with 40 levels in the vertical direction.

In the first case, about the internal treatment of carbon dioxide (CO_2), the CanESM2 model synthetically simulates CO_2 in the atmosphere in 3-dimensions, yearly cycle and year to year variability. The second case treats CO_2 fluxes in the ocean-atmosphere as well as land-atmosphere realms in an interactive way such that the simulated outputs can be used to identify certain emissions of CO_2, resulting from human activity, that match with certain global emission pathways.

CanESM2 model takes advantage of the ecosystem components in the terrestrial and oceanic realms which have been incorporated in the coupled global climate models (CGCMs). Such

CGCMs are able to simulate fluxes as well as evolutions for CO_2 together with a good number of GHGs in the ocean-land-atmosphere realms (Arora et al., 2009).

CanESM2 model outputs have been used the future in the future projection of north-south heat transport, terrestrial plant photosynthesis, various forms of climate elements such as extremes of temperature and precipitation through the process of downscaling (Arora et al., 2009; Feyissa et al., 2018; Keellings, 2016; Yang & Saenko, 2012).

2.6 Statistical Downscaling model (SDSM)

Statistical downscaling is a technique that finds out a relationship between local-scale predictand parameters and large-scale RCM or GCM outputs simulating synthetic data, making an assumption that such association remains into the future, and simulating synthetic data (Souvignet et al., 2010).

Numerous studies have been conducted using SDSM in downscaling GCM output products such as (Koukidis & Berg, 2010; Souvignet et al., 2010; Wilby, 2002).

Wilby and Dawson (2004) describe SDSM advantages and outline seven procedure steps followed in carrying out statistical downscaling using SDSM. According to the authors, SDSM is a powerful software tool that can be used for assessing the impacts of climate change at local scales. It is very user-friendly designed for downscaling GCM model outputs from course to finer resolution. It makes it possible to detect climate change signals which then can be applied more practically for assessment of climate change impacts at station-level scales. It can be used to facilitate rapid simulations of inexpensive, numerous, specific-site scenarios of surface meteorological conditions under current and future climate forcing. This computer application involves a number of steps including pre-screening of predictor variables, calibration of models, statistical analyses, elementary diagnostic testing and graphics of climate data. Application of SDSM follows seven steps (1) quality control and transformation of data, (2) predictor variable screening, (3) model calibration, (4) weather generator, (5) statistical analyses, (6) output from graphing model, and (7) generation of scenario (Wilby et al., 2004).

As described by Souvignet et al.(2010), SDSM is an hybrid result of transfer function and statistical-stochastic weather generator techniques (Souvignet et al., 2010) .

A study was conducted over Clutha river catchment in Sout Island, New Zealand by Hashni et al. (2009). The objective was to downscale precipitation and evaluate the level of uncertainties at local scale with the help of HadCM3-GCM model data outputs using SDSM, GEP, and LARS-WG models. The study involved an effort to downscale climate change signals under future climate scenario SRES A2. The authors found out that SDSM had a higher level of precision in downscaling standard deviation of precipitation unlike the normal cases where it is generally hard to do so by many downscaling models. The results for that study pointed out that SDSM slightly overestimated monthly precipitation just as much as it underestimated but the overall annual averages had no notable difference with the observed climate. Hashni et al. (2009) acknowledged that multi-model approach to quantification of uncertainties related to downscaled climate is appreciably efficient.

2.7 Research gap

There is scarcely any research study, from the available published literature, which has been conducted in Uasin-Gishu County to downscale GCM outputs to come up with daily Rainfall and temperature future scenario characteristics following different RCP radiative forcing. The current project, therefore, fills up the gap by using statistical downscaling model (SMSM) to downscale Canadian Second Generation Earth Systems Model (CanESM2) outputs under RCP4.5 and RCP8.5 in Uasin-Gishu County.

2.8 Conceptual Framework

The flow chart in the figure 3 below outlines the steps in the downscaling technique using SDSM. The process starts from acquisition of data both from for the meteorological station and the downscaling the model data under different RCP scenarios. After the acquisition, the data is subjected to quality control, then normalization where relevant, screening of predictors, model calibration, climate simulation and analysis.

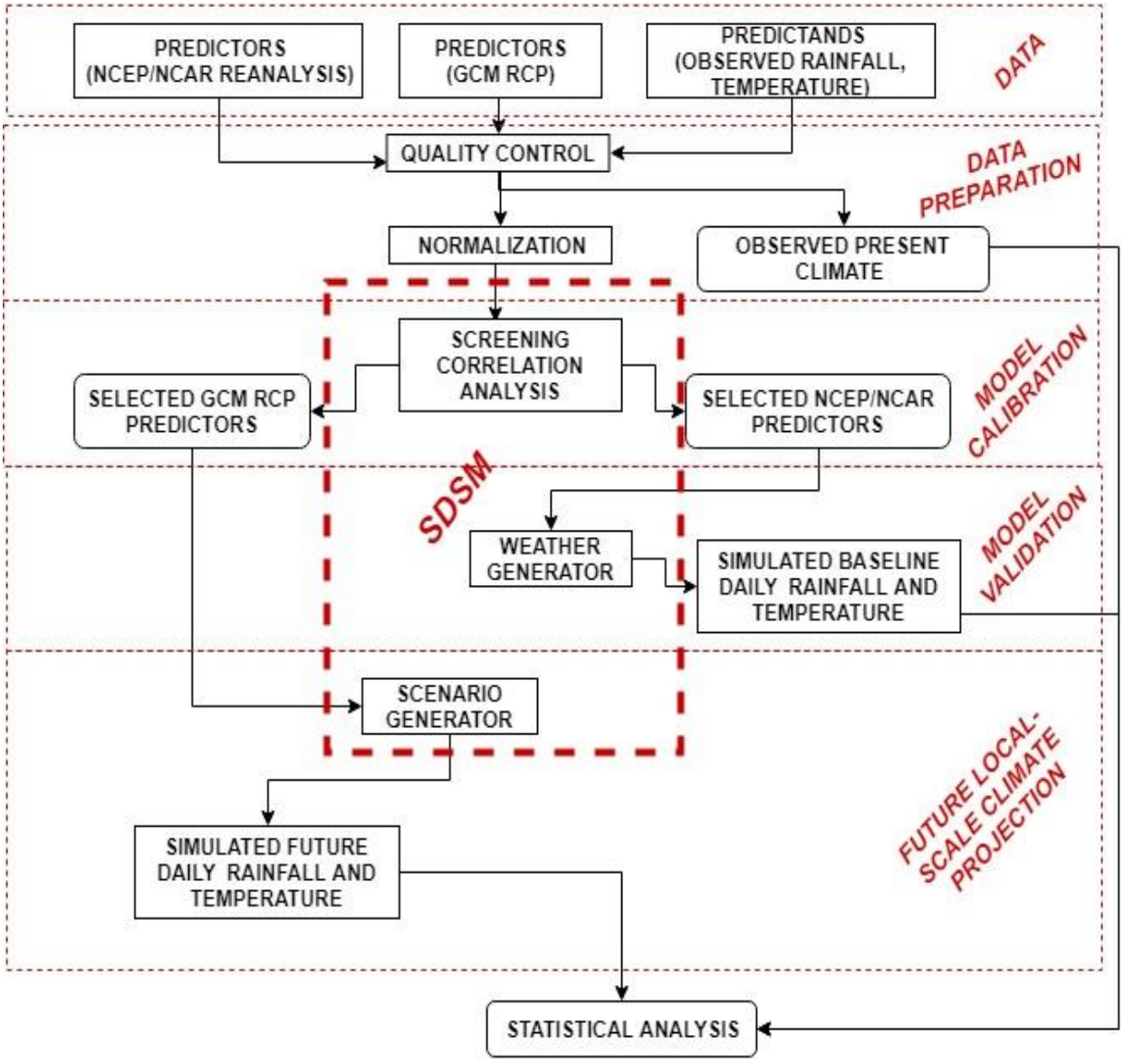

Figure 3: Conceptual framework

CHAPTER THREE

3.0 Data and Methodology

3.1 Data

In this study observed daily and monthly means of rainfall and temperature were used for the study. These data sets were obtained from the Kenya Meteorological Department for 45 years. Time period covered by the data ranged from 1st January 1974 through 31st December 2017 for Eldoret meteorological observation station. This station location is 0.404N and 35.239 E. The reason for acquiring monthly data was to be used in estimations of daily missing variables.

The daily climatic predictor dataset from the National Center for Environmental Predictions (NCEP) reanalysis were downloaded from available online on https://www.esrl.noaa.gov/psd/data/gridded/data.ncep.reanalysis.

Thirdly, the general circulation model (GCM) daily precipitation simulations will be obtained from the Coupled Model Inter-comparison Project phase five (CMIP5) climate change experiments from the year 2006 to 2100. CanESM2 model output data was used in the study, which is part of the coupled model inter-comparison project phase five (CMIP5), and is affiliated to the Canadian Centre for Climate Modeling and Analysis (CCCMA). This dataset is available online at https://esgf-node.llnl.gov/projects/esgf-llnl/. Table 2 and table 3 show different datasets used for the study.

Table 2: Datasets used in the study

Dataset	Temporal Resolution	Period	Source
Rainfall	Daily and monthly	1974-2017	Kenya Meteorological Department
Temperature	Daily and monthly	1974-2017	Kenya Meteorological Department
RCPs	Daily	2006-2099	Canadian Climate Data and Scenarios http://ccds-dscc.ec.gc.ca/?page=pred-canesm2
NCEP	Daily	1974-2005	Canadian Centre for Climate Modeling and Analysis (CCCMA)

Table 3: Predictor variables used for downscaling rainfall and temperature in the study

NCEP-NCAR Reanalysis Predictors	CanESM2 Model RCP Predictors	Description	Level	NCEP Code
ncepmslpgl.dat	ces2mslpgl.dat	Mean sea level pressure	Sea level	msl
Ncepp1_fgl.dat	ces2p1_fgl.dat	Airflow strength	surface	p1_f
ncepp1_ugl.dat	ces2p1_ugl.dat	zonal velocity	surface	p1_u
ncepp500gl.dat	ces2p500gl.dat	geopotential height	500 HPa	p500
ncepp850gl.dat	ces2p850gl.dat	Geopotential height	850 HPa	p850
ncepprcpgl.dat	ces2prcpgl.dat	Precipitation		prcp
nceps500gl.dat	ces2s500gl.dat	Specific humidity	500 HPa	s500
nceps850gl.dat	ces2s850gl.dat	Specific humidity	850 HPa	s850
ncepshumgl.dat	ces2shumgl.dat	Specific humidity	surface	Shum
nceptempgl.dat	ces2tempgl.dat	Mean temperature	surface (2m)	temp

3.2 Methodology

3.2.1 Estimating Missing Data

There is need to estimate missing data in any statistical analysis to ensure that the acquired data is of desired quality capable of guaranteeing sound interpretations from analysis. The process of filling up missing meteorological data sets often involves estimation using arithmetic mean, correlation and regression techniques.

In this study, simple arithmetic mean method was used. Each total monthly data was divided by the number of days in the month to fill up each of the daily missing data.

3.2.2 Homogeneity test for the observed climate

Data used in any research study must be subjected to quality analysis in order to ascertain that the output from the input of such information is sound for any particular application. As one of the ways to assess for the data quality, homogeneity test procedure was conducted to ensure that trends evident in the observed data sets were only as a result of the changes in the weather and climate conditions but not on the missing nor inappropriate measurements.

To test for homogeneity, single mass curves were plotted for the period covering the present climate (1973-2017). The single mass technique is done by plotting cumulative data against time.

3.2.3 Current climate analysis

Rainfall and average temperature conditions were analyzed for the period of 44 years from 1974 to 2017. Analysis was done for monthly, seasonal and inter-annual climate characteristics. Time series plots and trend analysis procedure was conducted both for the yearly and monthly climate parameters. In addition to this, seasonal trend, homogeneity and monotonic trend analysis was done as well.

To enable the analysis for any significant trends inherent in the datasets over time, Mann-Kendall statistical hypothesis test was used to determine the trend and seasonal homogeneity of the

datasets. Also, it was necessary to compute the difference in the means of two sample sets of different time periods.

Two-Sample Student t-test methodology was used in the analysis of two sample sets of climate parameters in order to quantify the amount of relative difference within 5% significance level. Density plots, box and whisker, and density plots were plotted and used to interpret the difference in means of the samples.

Monthly variabilities of the present climate were investigated using the coefficient of variation. Coefficient of variation is given by the standard deviation divided by long term monthly means and can be experienced as a percentage as was the case in this study. The results were tabulated and plotted.

3.2.4 Screening and selection of predictor variables

Having downloaded the NCEP-NCAR Reanalysis and the CanESM2 datasets, the task of screening and selection of the appropriate predictors from them started. Correlation analysis technique was used to establish how much of variabilities present in the predictands (rainfall and temperature) over time can be explained by the predictors (NCEP-NCAR Reanalysis predictors. The objective for doing so was to select those predictors that have the highest relationships with the predictand of interest.

The screening process used correlation technique to determine the empirical relationship between predictand(s) and the predictor(s). The method uses correlation coefficient, r, shown in equation 1. Correlation coefficient, r, quantifies the degree to which dependent is associated with independent variable in a linear relationship. The method is as follows:

$$r = \frac{\sum_{i=1}^{n}\left(x_i - \bar{x}\right)\left(y_i - \bar{y}\right)}{\left[\sum_{i=1}^{n}\left(x_i - \bar{x}\right)^2 \sum_{i=1}^{n}\left(y_i - \bar{y}\right)^2\right]^{1/2}} = \frac{n\sum xy - \sum x \sum y}{\sqrt{\left[n\sum x^2 - \left(\sum x\right)^2\right]\left[n\sum y^2 - \left(\sum y\right)^2\right]}} \quad \text{..... Equation 1}$$

Where *r* is the coefficient of correlation, *y* and *x* are the dependent and independent variables respectively, overbar indicates the mean, n is the sample size, *i* denotes each variable. coefficient of correlation is interpreted such that if *r*:

i. *r* is bounded by -1 and 1
ii. *r* being closer to -1 means a stronger negative correlation and a strongly positive otherwise.
iii. *r* is zero implies no correlation

The significance of the correlation coefficient can be determined using student-t test, coefficient of determination R^2, and *p*-value. Student-t test formula is shown in equation 2 below.

$$t_{n-2} = r\sqrt{\frac{n-2}{1-r^2}}, \quad \text{Equation 2}$$

Where n-2 = degrees of freedom, *n*=sample size, *r* = correlation coefficient, t_{n-2} = computed student-t statistic at *n-2* degrees of freedom. Coefficient of determination R^2 indicates the level of proportion in one variable that can be determined from a relationship with another variable. a p-value for a hypothesis test shows probability of the outcome is by chance. when p-value is very small the null hypothesis is rejected while the alternative hypothesis is accepted and vice versa. P-value statistical significance does not necessarily indicate an actual relationship but it just points out that the observed association is as a result of chance.

Observed data were reformatted into file formats readable to statistical downscaling model software (SDSM). Potential predictor variables such as sea level pressure, specific humidity, geopotential height, horizontal components of wind, among others were selected for use in the statistical model calibration.

3.2.5 Model calibration, validation and testing for skill

Model calibration process kick started after the selection of the most appropriate predictor variables. Methodology used in this case involved separating the observed climate datasets into two sample groups. The first sample from the year 1974 through 1995 were used to calibrate the

empirical-statistical model. The second sample for the period between the years 1996 to 2005 were retained for the verification of the model. Verification step involved comparison between the independent sample (1996-2005) and the data simulated for the same time period to determine how much the model can replicate the observed climate conditions.

It was necessary to apply the Two-Sample Student t-test to compare the differences between the means of the simulated and the observed data. The model was calibrated using the meteorological station observed predictors and the NCEP-NCAR reanalysis data in the statistical downscaling model software environment and stored in the chosen directory for the subsequent simulations.

For the model calibration, multiple regression technique was applied. Linear multiple regression model follows the formula in equation 3 below.

$$Y = \alpha + \beta X_1 - \gamma X_2 + \eta X_3 + \varepsilon \quad \text{..... Equation 3}$$

Where α, β and γ are coefficients such that the sum of residuals is as small as possible. Y is the dependent variable (predictand) and X (X_1, X_2, X_3) is the set of independent variables (predictor). ε (residual) is a random variable with zero as its mean.

Using SDSM, the monthly multiple regression models are computed through the least square technique by an optimization application program. This optimization algorithm calculates different multiple regression models for each month for every calendar year. Optimization algorithm in SDSM is capable of computing monthly, seasonal and annual multiple regression models. For the current study, we chose the monthly models. Also, SDSM application program does consider both conditional and unconditional model. Conditional model assumes there is a direct association of a predictor with some events whereas unconditional does not. In the present study, unlike temperature, we treated rainfall as a conditional preditand which depends on the events of wet days which in turn depend upon the GCM predictors like humidity.

The skill of the model was interpreted using the coefficient of determination (R^2), Durbin-Watson, Standard error and Chow statistics.

Durbin-Watson statistical test of hypothesis was used to explain the existence of autocorrelation in the prediction errors (residuals) for temperature in the statistical multiple linear regression analysis. The null hypothesis for the test is that there is no autocorrelation the lagged prediction errors (residuals). For the alternative hypothesis, there is autocorrelation. The bounds for the test is between 0 and 4. Whereas a value of two means there is no autocorrelation, anything less or more points out to a positive and negative correlation respectively. Presence of negative correlation is indicated by a value more than two. If the value is less than one, it means there is a serial positive auto-correlation and there is a reason to worry. The formula for Durbin-Watson Statistic is shown in equation 4.

$$d = \frac{\sum_{t=2}^{T} (e_t - e_{t-1})^2}{\sum_{t=1}^{T} e_t^2}, \quad \text{Equation 4}$$

Where T is the observation sample size, e_t is the residual error related to time of observation (t) and d is the Durbin-Watson statistic.

3.2.6 Downscaling of the future climate under RCP scenarios

As was indicated in the problem statement of the rationale informing this study, the coarser-resolution general circulation model datasets necessitated the need for downscaling into a finer station-level scale. This is so that the local climate phenomena can be examined over a smaller area of a given locality. Downscaling makes it possible to check for the presence of the climate change signal that has been witnessed over global and regional scales by climate change modelers.

The principle behind the statistical downscaling used in this study is based on the assumption that the established statistical-empirical relationships inherent between the large scale predictor (reanalysis remote sensed and modelled) climate variables and the station-level predictors (observed) continue to hold into the future.

Using the statistical models developed for each predictand for each month from the calibration stage, simulations were carried out in the SDSM version 4.1 software environment. Rainfall and temperature datasets were generated using the NCEP-NCAR predictors for the period to be used for model verification. Scenario generator tool, in the SDSM package, was used to synthesize climate conditions under RCP 4.5 and RCP 8.5. The simulated climate at the station-level resolutions was ready for analysis and possible applications.

3.2.7 Analysis of future climate characteristics

The last step in the statistical downscaling we conducted involved subjecting the simulated climate conditions into various techniques of analysis. It also dealt with the comparisons between the near-term period simulated and the present climate datasets. A consideration was made to distinctly separate the downscaled data under RCP 4.5 and RCP 8.5.

Future climate analysis involved comparisons of the observed (1980-2009) and the near-term downscaled (2010-2039) datasets using the two-sample student-t test of hypothesis at 5% significance level. The procedure for this hypothesis extended to plotting the dot density, box and whisker, and the density plots to be used in farther assertions of the statistical results.

Time series and trend analysis techniques were also applied at this stage. Yearly totals of the daily downscaled climate data were plotted against time. Trends present in the data over time were investigated using the Mann-Kendall statistical test at 95% confidence interval. While determining possible trends in the time series plots, it was not enough to consider the p-value probabilities alone but to proceed and use the computed slope estimator. In the event, the p-values showed no Significant trend, the value of the slope estimated, which indicates the magnitude of the increasing (positive) and decreasing (negative) trends, were used to judge the direction of the trend.

In the period from the year 2010 to 2039 (near-term period), we analyzed the annual as well as seasonal time series and trends exhibited by the simulated climate. Monthly seasonal trends and homogeneity tests were conducted using the SYSTAT statistical package version 13. Using the statistical software, Mann-Kendal Test of hypothesis to test for trends and homogeneity was used.

CHAPTER FOUR

4.0 Results and Discussions

Results and discussions are discussed in this section.

4.1 Homogeneity Test

The results for homogeneity test are shown and discussed in this subsection. Figure 4 shows the single mass curve for rainfall for the year1974 to 2017. The curving up around 1984 could be attributed to the findings by Ininda et al. (2008) and Huho and Mugalavi (2010). 1984 among other list of years was one of the driest years in the lake Victoria basin region (Ininda et al., 2008). A drought with a severity index of negative 2.78 occurred in the Rift Valley environments between the year 1984 to 1985 (Huho & Mugalavai, 2010). Around 1984, therefore, was a significant decrease in rainfall occurrence around the study area.

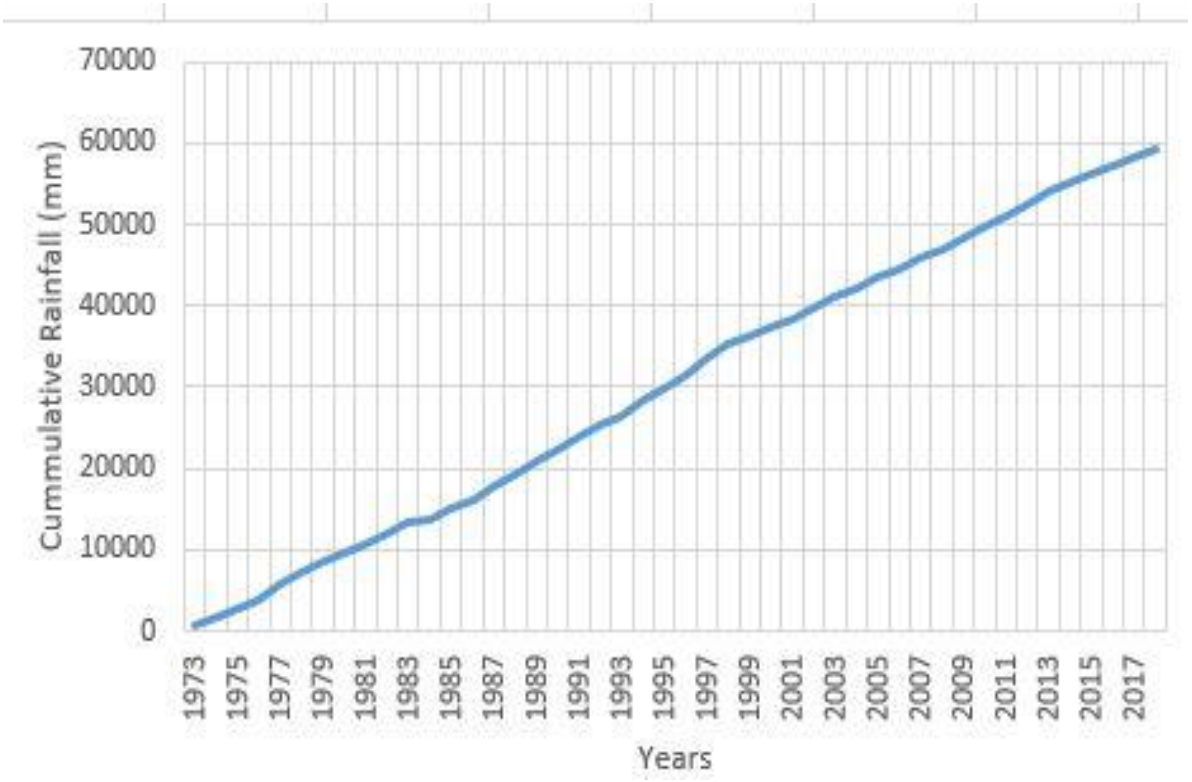

Figure 4: Single mass curve for observed rainfall for the period 1974-2017

Figure 5 depicts homogeneity result for the average temperature from the year 1974 to 2017. The plot indicates that the observed temperature data was quite homogeneous as the line is fairly straight. This points out to the most probable likelihood that the temperature data acquired for use in this project originated from a common population. Homogeneity, in this case, shows that the changes observed in temperature over time is most likely due to changes in the climate conditions and not due to changes in the methods of observations and the associated instruments.

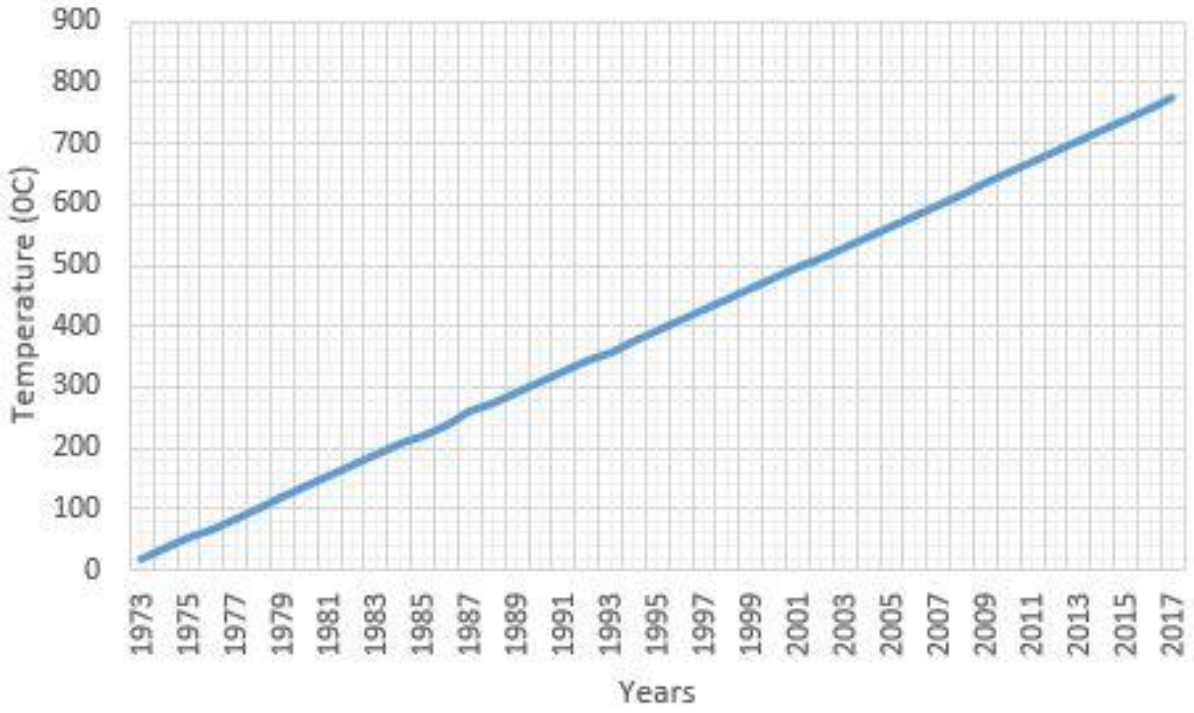

Figure 5: Single mass curve for observed average temperature for the period 1974-2017

4.2 Current Climate Analysis

Current climate analysis results are shown in this sub-section.

4.2.1 Monthly Distributions and Variations of climate conditions

The averages of the monthly rainfall and temperature were determined from the data obtained from the Kenya Meteorological Department observed from 1974 to 2017 as shown in figure 6. The monthly distributions of rainfall over Eldoret show two main wet seasons: March-May (MAM)

and June-Aug (JJA) with peaks in April and August respectively. On average, Eldoret receives the highest amount of rainfall in the month of August.

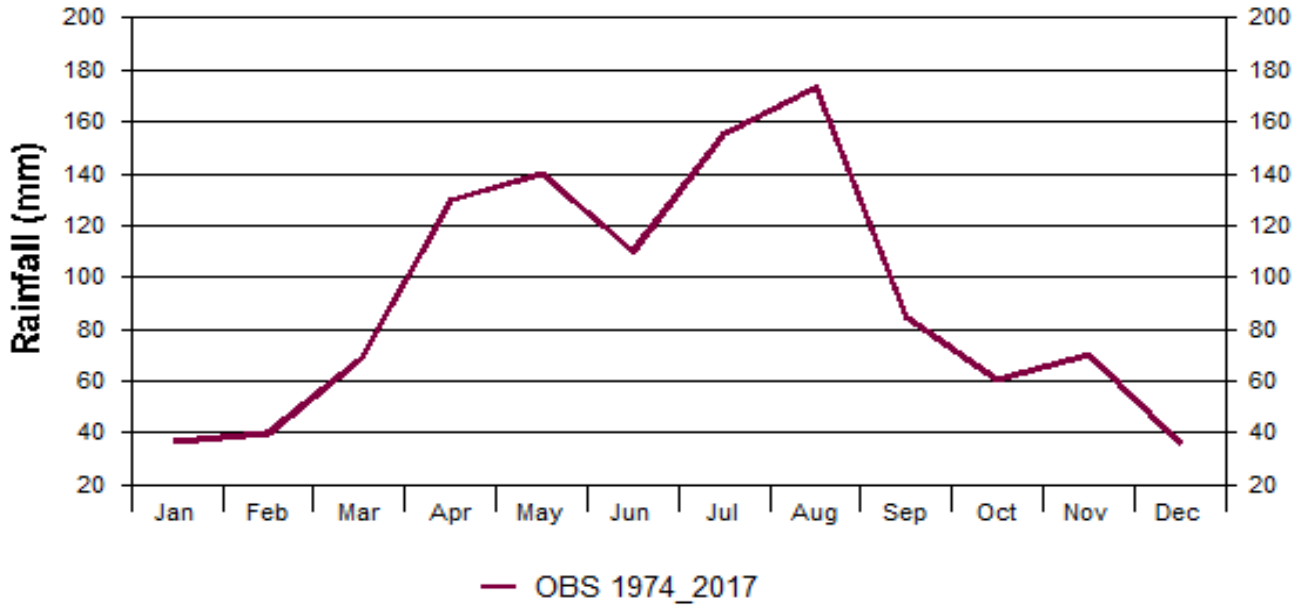

Figure 6: Mean Monthly Rainfall (mm) from 1974-2017

Figure 7 shows the monthly temperature variations in the study area. From the analysis, temperatures are at highest in March and lowest between July and August.

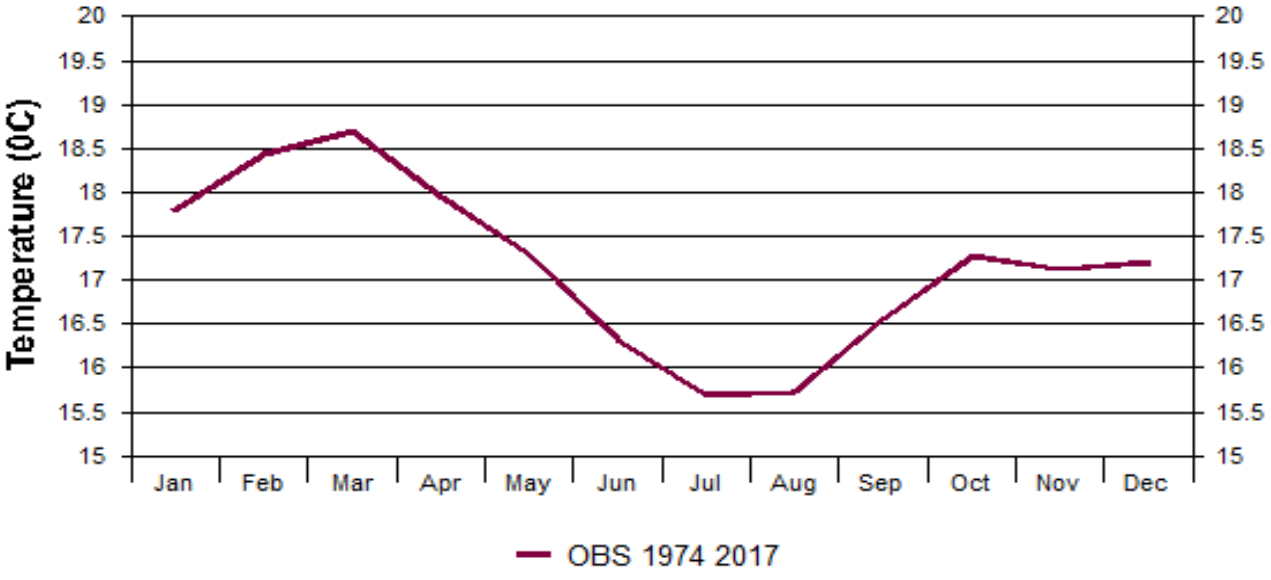

Figure 7: Mean Monthly Average Temperature (^{0}C) from 1974-2017

For each month, variability of rainfall and average temperature is explained by means of coefficient of variation (CV) as in figure 8 and figure 9 respectively. CV is defined by dividing the standard deviation by the long term monthly average. December and July are the months with the highest and the lowest rainfall variability respectively. From figure 8, much of the rainfall variability (CV>50%) happens in the period of January-March and September to December. Climatologically, December-February (DJF) is the season with the most rainfall variability. For the entire period (1974-2017) the long term monthly average temperature indicate low variabilities (CV< 7%) as shown in figure 9. The lowest temperature variability occurs in March and highest happens around July and August.

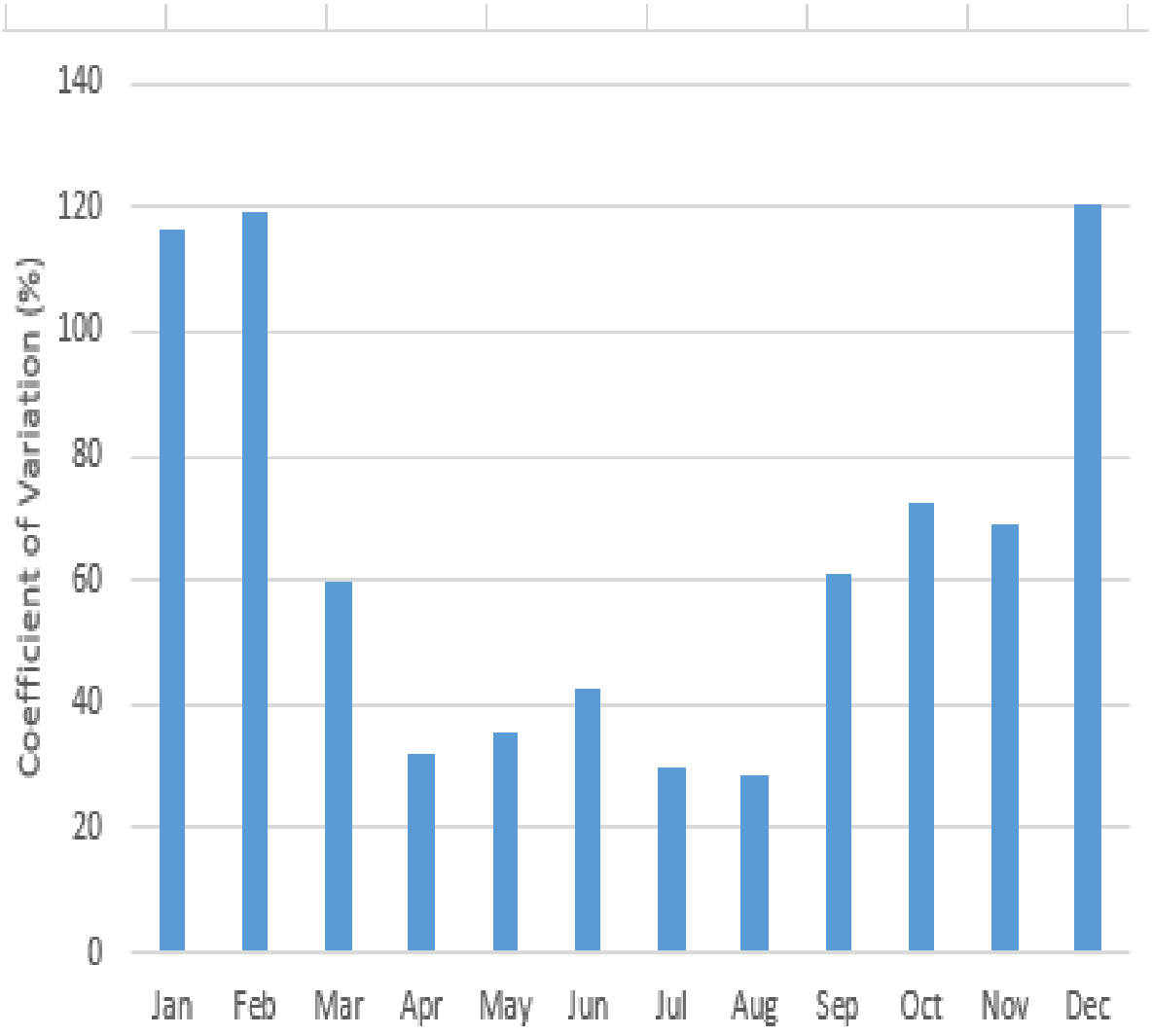

Figure 8: Variability of rainfall month by month shown by the coefficient of variation (%).

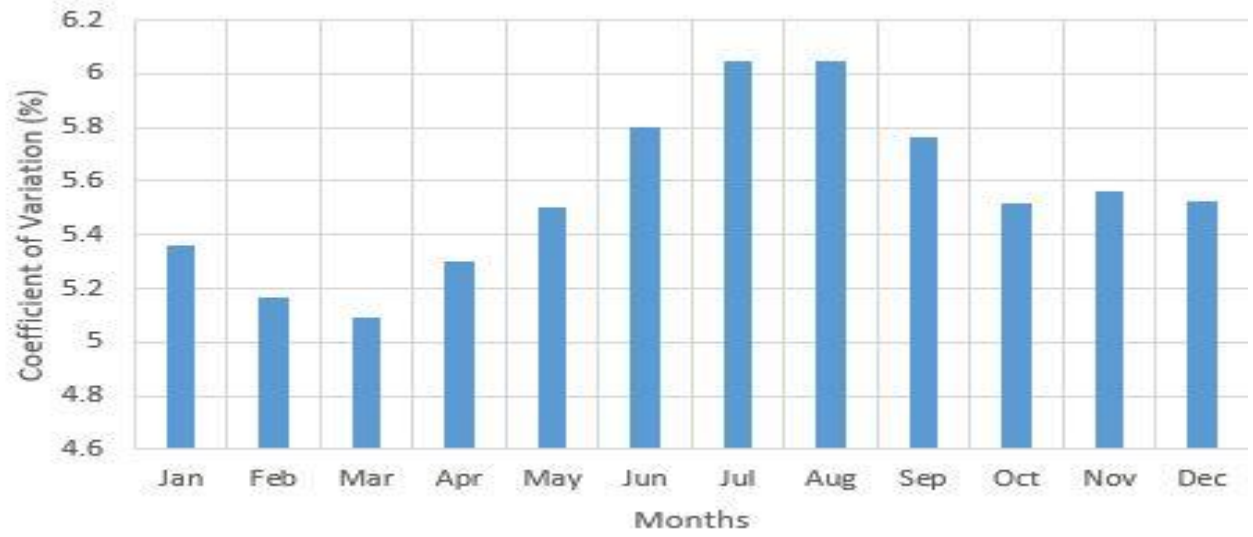

Figure 9: Variability of average temperature month by month shown by the coefficient of variation (%).

4.2.2 Time Series and Trend Analysis

For the entire period from 2006 to 2099, the simulated RCP climate variables were plotted as shown in figure 10 and figure 11. Figure 10 and figure 11 show upward trends for the observed rainfall and temperature respectively.

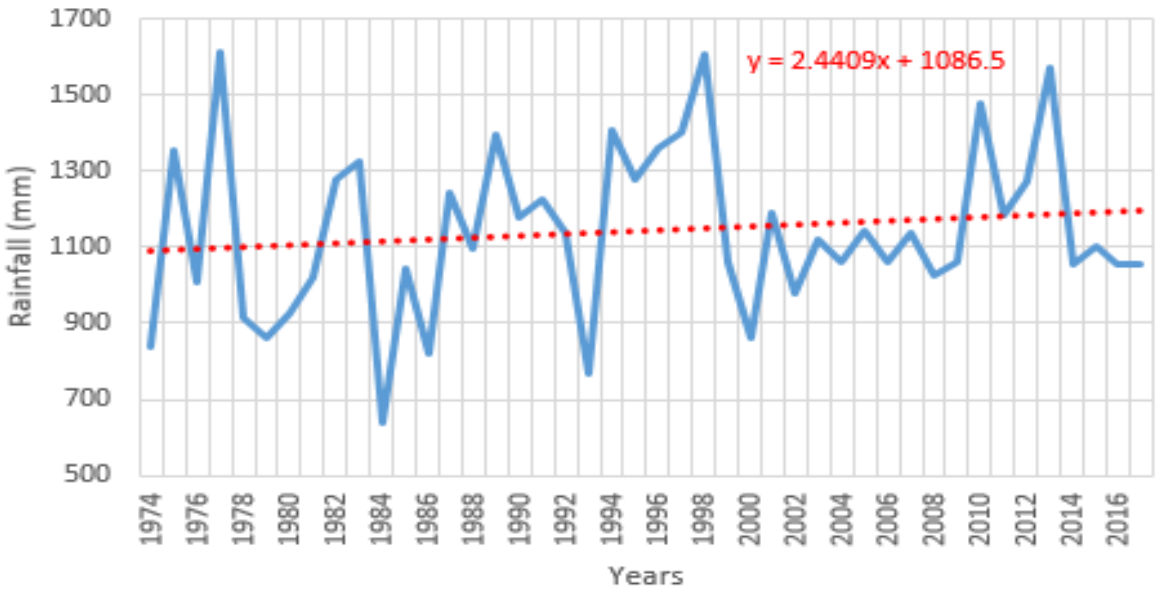

Figure 10: Time series for observed rainfall 1974-2017

The equations for the trend-lines show positive increments of approximately 2.4 and 0.01for rainfall and temperature respectively.

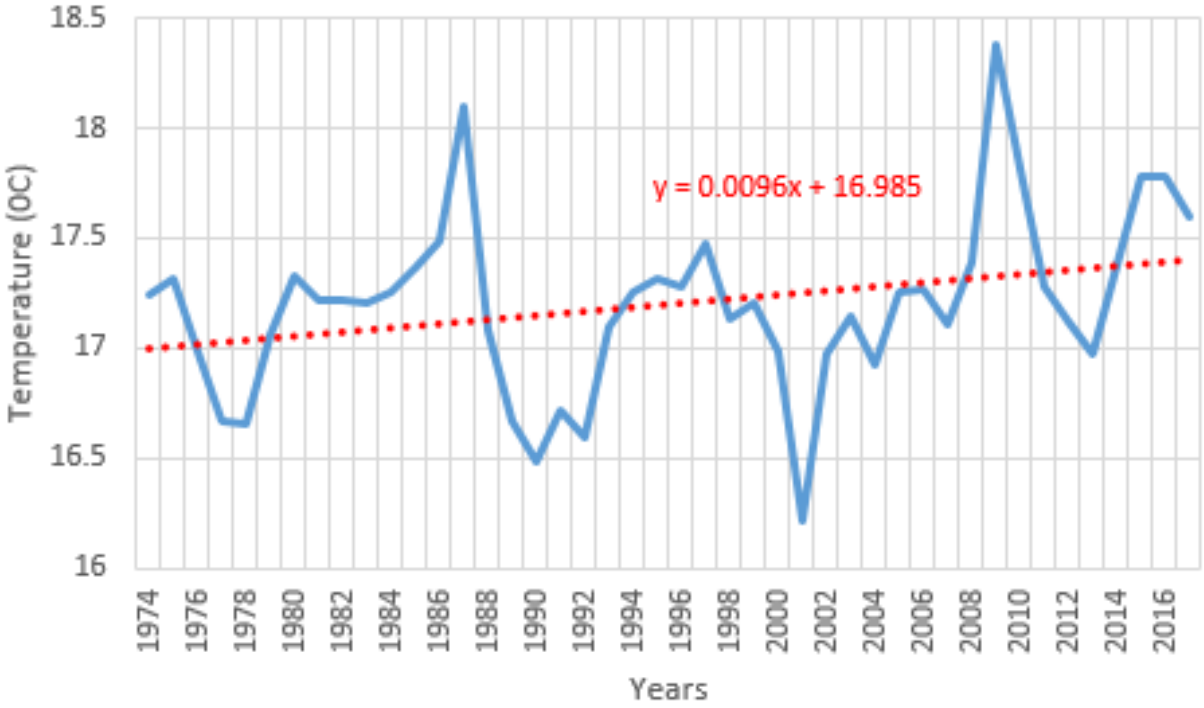

Figure 11: Time series for observed average temperature 1974-2017

Trend test for rainfall and average temperature time series was examined using the Mann-Kendall statistical test. In order to use the test statistic, a null (H_0) and alternative (H_1) hypotheses were formulated as follows:

H_0: No Trend vs. H_1: Upward Trend

In the period 1974-2017, the hypothesis test statistics and p-values were computed at 95% confidence interval. Notice that for rainfall, the Mann-Kendall test p-value (0.215) in table 4 does not indicate significant increasing trend. However, the slope estimate (2.295) indicates the magnitude of the upward trend. From the slope estimate of 2.292 mm/year, a corresponding decadal rate of rainfall increment is 22.92 mm/decade. The average temperature Mann-Kendall p-value (0.029), in table 4, signals a significant warming at the rate of 0.008 ^{o}C/year (slope estimate=0.008) translating to an upward trend of 0.08 ^{o}C/decade.

Table 4: Mann-Kendall test results for the climate variables in the period 1974-2017

Variable	Statistic	ASE	Z	p-Value	Slope Estimate	95% Lower Limit	Tau Statistic
Rainfall	79	98.865	0.789	0.215	2.295	-2.345	0.084
Average Temperature	188	98.870	1.891	0.029	0.008	0.001	0.199

Z= Mann Kendall Z statistic

Two-sample student-t hypothesis test was applied to compute the differences between two sample splits (1974-1995/1996-2017) for the climate variables at 5% significance level. The null and alternative hypotheses formulated were such that:

H_0: Mean A = Mean B vs. H_1: Mean A <> Mean B (Mean A is not equal to Mean B)

Rainfall and average temperature datasets were classified as data B (1974-1995) and data A (1996-2017) and then hypothesis test computed. Results are shown in table 5 and table 6. The results for the dot density, box and whisker, and density plots are depicted by figure 12 and figure 13. The p-value (0.33) in table 6 indicates a significant inequality between the average mean for rainfall for the two samples used for testing. Upon examining the dot density, box and whisker, and density plots in figure 12, we see that on average, the mean for Data A (1996-2017) is higher than that of Data B (1974-1995) by approximately 5.6%. In the case of temperature p-value (0.124) from table 3 points to a significant increase over time (1974-1995/1996-2017). Dot density, box and whisker, and density plots in figure 13 confirm the significant difference in the samples. The mean difference is about 1.1% increase for the same time period and sample splits.

Table 5: Student-t hypothesis test for the two climate samples (1974-1995/1996-2017)

	Variable	N	Mean	Standard Deviation	Mean Difference (A-B)	Mean difference (%)
Rainfall	Data A	22	1,174.42	194.728	65.977	5.617837
Rainfall	Data B	22	1,108.45	246.4		
Temperature	Data A	22	17.294	0.424	0.188	1.0871
Temperature	Data B	22	17.107	0.367		

N=Sample Size

Table 6: Separate and pooled variance results for the two samples of climate variables

	Variable	Mean Difference (A-B)	95% Confidence		t	Degrees of freedom	p-Value
			Lower Limit	Upper Limit			
Separate Variance (Rainfall)	Data A	65.977	-69.362	201.317	0.985	39.871	0.330
	Data B						
Pooled Variance (Rainfall)	Data A	65.977	-69.148	201.103	0.985	42.000	0.330
	Data B						
Separate Variance (Temperature)	Data A	0.188	-0.054	0.429	1.571	41.170	0.124
	Data B						
Pooled Variance (Temperature)	Data A	0.188	-0.053	0.429	1.571	42.000	0.124
	Data B						

t=Student-t statistic, *p*-value=computed probability used for accepting or rejecting the null hypothesis.

Dot density, box and whisker, and density plots were also graphed to help in cross-checking the validity the two-sample student t-test.

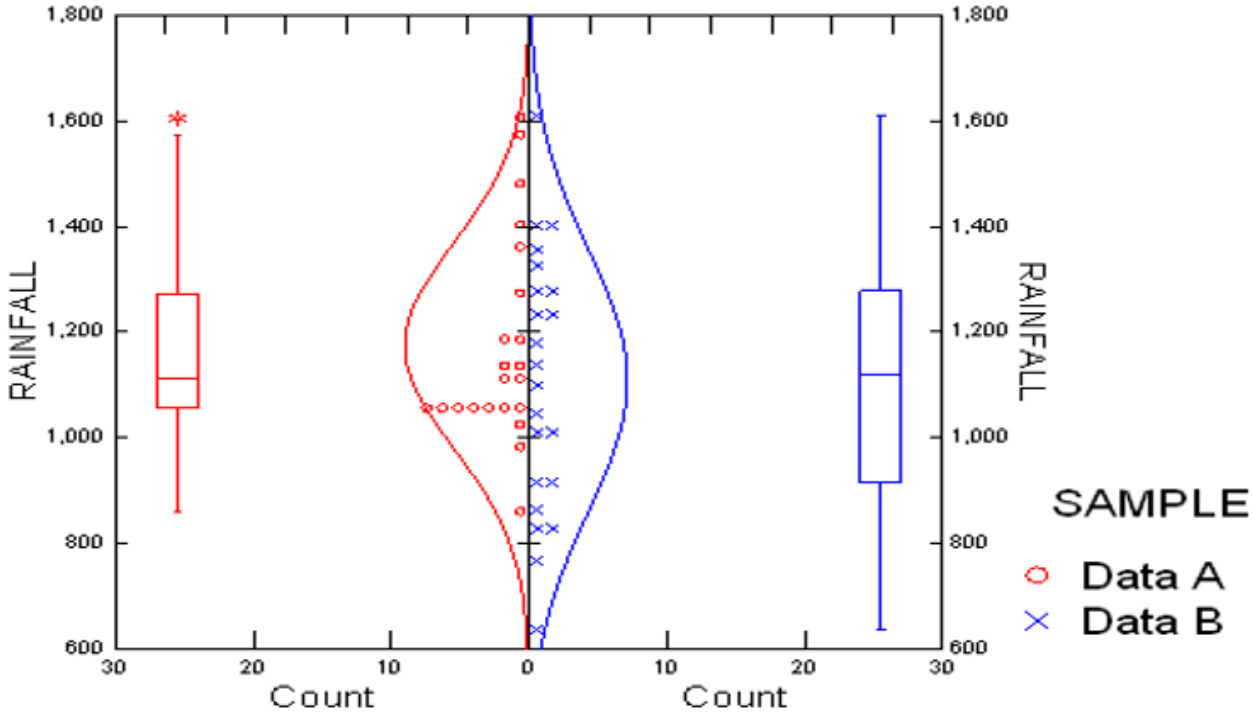

Figure 12: Dot density, box and whisker, and density plots for two Rainfall samples (1974-1995/1996-2017)

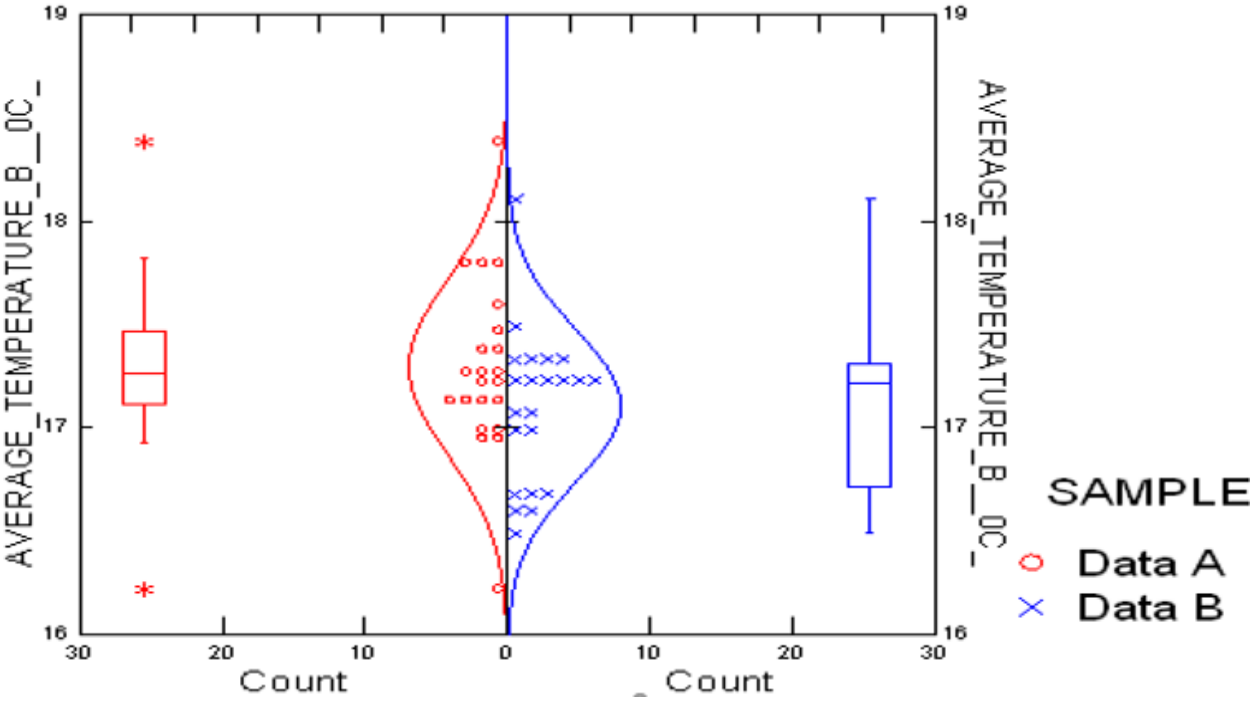

Figure 13: Dot density, box and whisker, and density plots for two average temperature samples (1974-1995/1996-2017)

On examining the annual averages of two samples of rainfall and average temperature over a period of 21 years (1974-1995/1996-2017), an upward trend is revealed. Table 7 shows a significant increase of about 5.6% for rainfall in the two periods. The student t-test statistical significance (p-value 0.835) about the increase is shown in table 8. Student t-test null and alternative hypothesis are such that:

H0: Mean A = Mean B vs. H1: Mean A > Mean B

Table 7: Hypothesis testing of 1974-1995 and 1996-2017 rainfall inter-annual samples

Variable	Number of cases	Mean	Standard Deviation	Relative change (%
Sample A (1974-1995)	22	1,108.45	246.4	5.617849
Sample B (1996-2017)	22	1,174.42	194.728	

Table 8: Separate variance of the 1974-1995 and 1996-2017 rainfall inter-annual samples

Variable	Mean Difference (A- B)	95% Confidence Bound	t statistic	Degrees of freedom (df)	p-value
Sample A (1974-1995)	-65.977	-178.732	-0.985	39.871	0.835
Sample B (1996-2017)					

4.2.3 Rainfall seasonal trend analysis

Seasonal time series plots for the MAM, JJA, SON and DJF seasons are shown in figure 11.

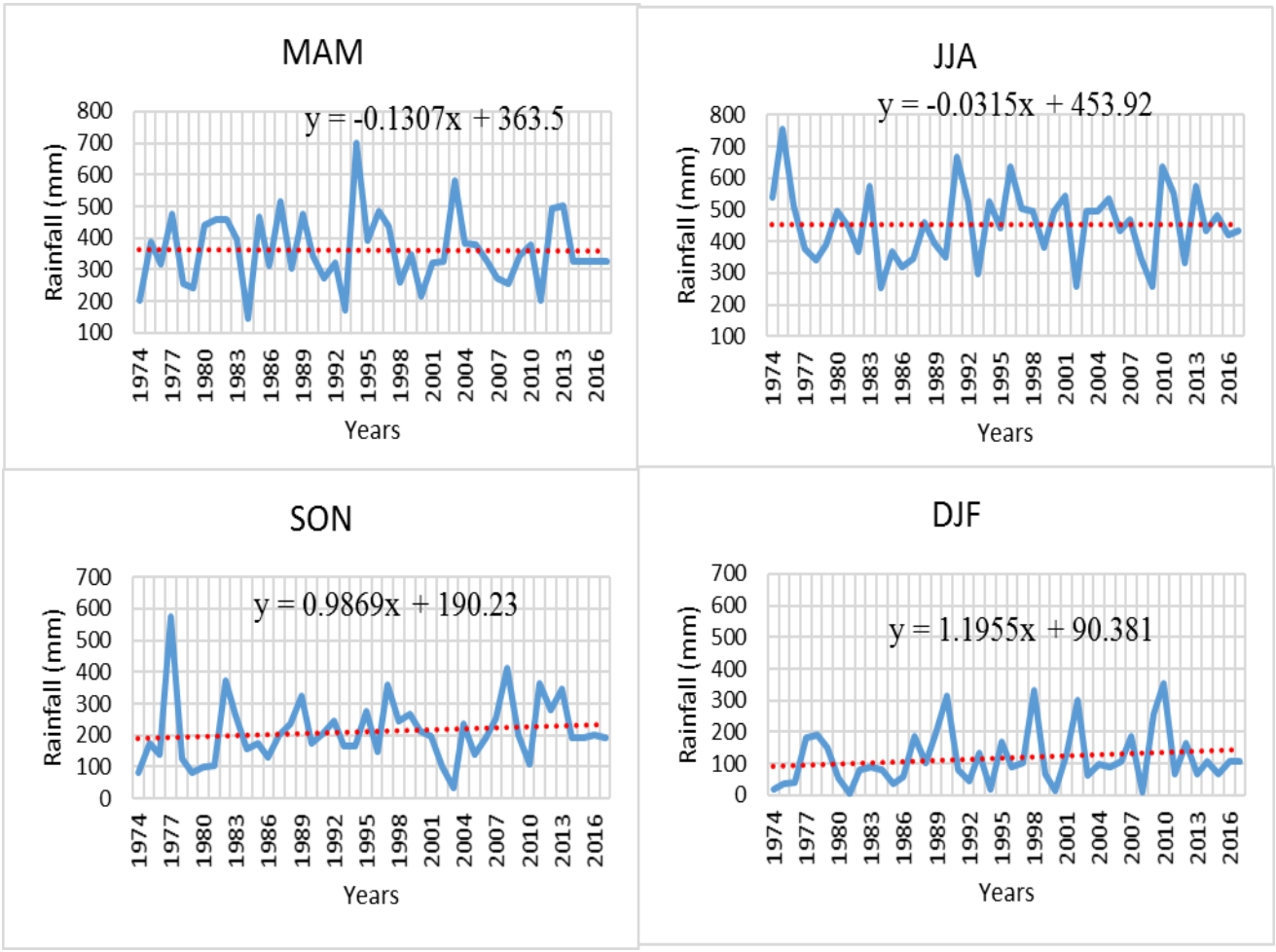

Figure 14: Seasonal time series trend plots

The time series for the seasons were farther analyzed for any indication of trend. The possible trend season by season were investigated by applying the Mann-Kendall Test.

Table 9: Mann-Kendall Statistic for the four Seasons (MAM, JJA, SON, DJF)

Season	Number of observations	Statistic	ASE	Tau
MAM	44	-3	98.821	-0.003
JJA	44	7	98.767	0.007
SON	44	164	98.826	0.173
DJF	44	147	98.808	0.155

MAM=March-May, JJA=June-July, SON=September-November, DJF=December-February

So as to test for seasonal Kendall test, null (H_0) and alternative (H_1) hypotheses were formulated, tested and the results shown in table 9 and table 10:

H_0: No Trend vs. H_1: Upward Trend

The seasonal and modified Kendall test p-values (0.055 and 0.057) in table 10 do not indicate a significantly increasing general seasonal trend. However, the slope estimator (0.753) in table 11 gives the magnitude (slope) of the upward trend present in the seasonal datasets.

Table 10: Seasonal Kendall test and p-value at 95% confidence interval

Seasonal Kendall Test	Statistic	ASE	Z	p-Value
	315.000	197.612	1.594	0.055
Modified Seasonal Kendall Test	Statistic	ASE	Z	p-Value
	315.000	199.318	1.580	0.057

Table 11: Seasonal Kendall Tau Statistic and the estimated slope

Seasonal Kendall Test	Slope Estimate	95% Lower Limit	Kendall Tau Statistic
	0.753	0.000	0.083
Modified Seasonal Kendall Test	Slope Estimate	95% Lower Limit	Kendall Tau Statistic
	0.753	0.000	0.083

4.2.4 Rainfall Seasonal Homogeneity and Monotonic Trend Analysis

Two tests of hypothesis corresponding to homogeneous and trend test were formulated before and then statistics calculated as follows:

H_0: Homogeneous Seasonal Trend vs. H_1: Non Homogeneous Seasonal Trend

H_0: No Trend vs. H1*: Presence of Monotonic Trend

The results for the hypotheses are shown in table 12 and table 13. From the p-value (0.488) in table 12 which corresponds to the homogeneity in the homogeneity test, there is a notable homogeneous upward trend over time. Having confirmed homogeneity, we opt for general seasonal monotonic

trend. The p-value (0.111) in table 12 corresponding to the trend in the homogeneity test does not indicate any significant overall seasonal-monotonic trend throughout time.

Table 12: Seasonal trend and homogeneity test results

	Statistic	Degrees of freedom (df)	p-Value
Homogeneity	2.433	3	0.488
Trend	2.54	1	0.111
Total	4.973	4	0.29

4.3 Screening of Predictor Variables

The process of screening for most probable predictors for rainfall and temperature culminated with the results in tables 13 and 14 below. Tabulated results give the explained variance by each of the selected NCEP and CanESM2 model predictor variables.

Table 13: NCEP predictors explained variance results for rainfall and temperature with at 5% significance level from 1/1/1974 to 31/12/1995

Rainfall												
Predictors	JAN	FEB	MAR	APR	MAY	JUN	JUL	AUG	SEP	OCT	NOV	DEC
ncepmslpgl.dat	0.083	0.05	0.03	0.01	0.03	0.03	0.02	0.01	0.03	0.03	0.06	0.07
ncepp500gl.dat	0.200	0.081	0.073	0.035	0.066	0.052	0.047	0.049	0.069	0.098	0.059	0.063
ncepp850gl.dat	0.119	0.051	0.055	0.013	0.038	0.031	0.020	0.022	0.038	0.039	0.050	
nceps500gl.dat	0.012	0.015	0.013				0.021		0.012	0.042		0.041
nceps850gl.dat	0.020	0.013		0.010			0.028	0.024			0.019	0.035
ncepshumgl.dat	0.019	0.013			0.010	0.010	0.027	0.021	0.008		0.039	
Temperature												
Predictors	JAN	FEB	MAR	APR	MAY	JUN	JUL	AUG	SEP	OCT	NOV	DEC
ncepmslpgl.dat	0.017	0.015		0.046	0.010	0.016	0.013	0.027	0.015	0.010		0.043
Ncepp1_fgl.dat			0.008	0.014					0.012			
ncepprcpgl.dat	0.018			0.037	0.009	0.034	0.012	0.011	0.016	0.015	0.008	
ncepshumgl.dat	0.012			0.045		0.015	0.013		0.015	0.010		
nceptempgl.dat	0.032			0.036	0.012	0.011					0.011	

Table 13 shows the results for the different NCEP predictors selected for the model calibration during the screening process. The values in the table indicate the level of variance in the predictand that can be explained by the potential predictors.

Table 14: CanESM2 predictors explained variance results for rainfall and temperature with at 5% significance level from 1/1/1974 to 31/12/1995

Rainfall												
Predictors	JAN	FEB	MAR	APR	MAY	JUN	JUL	AUG	SEP	OCT	NOV	DEC
ncepmslpgl.dat		0.009									0.050	
ncepp500gl.dat					0.018	0.019				0.066	0.014	
ncepp850gl.dat									0.008	0.040	0.009	
nceps500gl.dat				0.010	0.027						0.012	
nceps850gl.dat				0.019	0.027	0.018			0.012	0.042	0.019	
ncepshumgl.dat				0.021	0.027	0 .017			0.009	0.047	0.057	
nceptempgl.dat		0.008		0.011						0.054		
Temperature												
Predictors	JAN	FEB	MAR	APR	MAY	JUN	JUL	AUG	SEP	OCT	NOV	DEC
ncepmslpgl.dat						0.012		0.024		0.022		
Ncepp1_fgl.dat		0.019										
ncepprcpgl.dat			0.010									
ncepshumgl.dat			0.008			0.008		0.011				
nceptempgl.dat	0.007					0.037		0.021		0.012		

The mean sea level pressure and 500 hpa geopotential height can explain variances for rainfall for every of the months in the year. Compared to all the predictors, the results indicate that geopotential height at 500 hpa level is the most probable predictor for rainfall. It can account for variance the most for all months compared to the other predictors except November and December. For November (0.05) and December (0.07), the mean sea level pressure is arguably the most important predictor for downscaling rainfall. The 850 hpa geopotential height also is quite efficient in accounting for variabilities present in rainfall except for December.

Still in table 13, NCEP precipitation and mean sea level predictors can account for variances in the observed temperature for over 9 months in a year for the entire screening period. In the case of temperature, the most possibly important predictor is the mean sea level pressure. Only in the month of April do all of the predictors account for variabilities of temperature. None of the predictors for temperature is potentially fit for use in model calibration in March and December except for the surface airflow strength and mean sea level respectively.

For the CanESM2 predictors, table 14 contains the explained variances. The months in which negligible amounts of explainable variances for rainfall by the CanESM2 predictors are January, March, July, August and December. In February, CanESM2 mean sea level pressure is the most probable predictor for rainfall. The near surface specific humidity is the most important predictor

for rainfall especially for April, May, September and November. For the June and October, the best CanESM2 predictor is the geopotential height at 500 hpa level.

The best predictors for observed temperature in January and June, February, March, June, August and October are temperature, airflow strength, precipitation and mean sea level respectively. There is hardly any temperature variance explainable by the NCEP predictors for April, May, July, September, November and December.

4.4 Model Calibration, Validation and Skill Testing

After accomplishing the mission for predictor selection, a multiple linear regression for each month was calibrated in SDSM environment for the period from the year 1974 to1995. The model was then subjected to validation and its skill tested as well. A section of the observed data in the years ranging from 1996 to 2005 was left out purposely for use in analyzing the ability of the model to simulate the observed climate conditions. Results for this section are shown in table 15, table 16, table 17 and table 18.

Table 15: Conditional model calibration statistics for rainfall NCEP predictors 1/1/1974 to 31/12/1995

Month	Coefficient of determination (R^2)	Standard error (SE)	Chow
January	0.080	2.177	**5.8127**
February	0.132	2.301	**10.7916**
March	0.034	2.658	**3.0550**
April	0.063	2.960	**8.1978**
May	0.082	2.428	**4.7465**
June	0.017	2.256	**5.9295**
July	0.019	2.522	**3.5330**
August	0.017	3.749	**2.9582**
September	0.001	1.370	**2.4686**
October	0.025	4.823	0.4718
November	0.162	3.650	**8.3593**
December	0.012	0.914	**4.0775**

Table 16: Conditional model calibration statistics for rainfall CanESM2 predictors 1/1/1974 to 31/12/1995

Month	Coefficient of determination (R^2)	Standard error (SE)	Chow
January	0.007	2.207	-0.2379
February	0.015	2.360	1.7511
March	0.018	2.672	1.8376
April	0.023	2.966	1.6817
May	0.012	2.519	**4.1589**
June	0.016	2.256	**5.8567**
July	0.015	2.523	**2.2976**
August	0.001	3.798	**3.9462**
September	0.010	1.364	**2.0955**
October	0.000	4.856	0.3304
November	0.002	3.818	-1.0108
December	0.016	0.912	**3.0047**

Table 17: Unconditional model calibration statistics for temperature NCEP predictors 1/1/1974 to 31/12/1995

Month	R^2	Standard error (SE)	Chow	Durbin-Watson
January	0.030	1.027	**8.2413**	1.156
February	0.001	0.909	**9.7656**	1.432
March	0.015	0.999	**8.3795**	1.125
April	0.067	0.769	**8.5283**	1.163
May	0.030	0.830	**12.0225**	1.253
June	0.044	0.827	**10.8777**	1.169
July	0.017	0.752	**7.5516**	1.705
August	0.028	0.773	**4.9518**	1.346
September	0.021	0.833	**9.0660**	1.608
October	0.000	0.892	1.9829	1.428
November	0.009	0.801	0.6791	1.471
December	0.001	0.759	**2.1637**	1.635

In order to examine the skill of the calibrated model to synthesize the observed conditions coefficient of determination (R^2), standard error (SE), Chow and Durbin-Watson statistics were computed at 95% confidence interval and results recorded in tables 15 to 18 above. The standard error (SE) is just but the standard deviation of differences between the predictor (rainfall or temperature) and the predictors (normalized NCEP) for the period 1974 to 2005.

Table 18: Unconditional model calibration statistics for temperature CanESM2 predictors 1/1/1974 to 31/12/1995

Month	R^2	Standard error (SE)	Chow	Durbin-Watson
January	0.002	1.110	-12.9380	1.281
February	0.000	0.906	**6.2747**	1.432
March	0.009	0.998	**8.1723**	1.123
April	0.004	0.777	**6.3201**	1.138
May	0.001	0.831	**9.4698**	1.251
June	0.034	0.833	**9.9082**	1.169
July	0.001	0.749	**6.3800**	1.717
August	0.000	0.771	**6.7380**	1.350
September	0.002	0.835	**5.9402**	1.598
October	0.000	0.893	**2.3600**	1.426
November	0.002	0.802	0.3628	1.469
December	0.000	0.755	1.4125	1.651

For rainfall, SE values in table 15 and 16, are higher (between 2 and 4.9) than for the case of temperature. December (<1) has the least and October (about 4.8) the largest SE for rainfall. This suggests that the NCEP predictors can predict rainfall to a larger extend in December and lowest in October. From tables 17 and 18, SE most of the values for temperature are very low (<1) suggesting a high level of the linear relationship between the observed temperatures and the selected CanESM2 and NCEP predictor variables.

As for the results in tables 17 and 18 for Durbin-Watson test all the values are ranging between 1 and 2 and no value is less than 1. The implication for this is that it is most probable that independence assumption is conserved for the temperature residuals (prediction errors) in the regression analysis.

In the current study, Chow statistical test was applied to test if coefficients for two linear models developed from two samples of the same population are equal. The null hypothesis for Chow is that coefficients in two linear models are equal otherwise the alternative hypothesis is defined. The reason for using the Chow test is to determine if an individual regression line or two can best fit the data in a time series. The results for rainfall in table 15 and 16 show that coefficients of the models used to predict rainfall are notably the same for all the monthly models using NCEP predictors except in October as shown in bold. Using the CanESM2 predictors, the rainfall monthly

regression models can only have the same coefficients in May to September and December. As shown in bold in table 17, the NCEP predictors perform very well in predicting the temperature through linear monthly regression model for all the months except December. Using CanESM2, the models for temperature are skillful except in November and December.

Simulated and observed climate parameters that were not used in the model calibration were analyzed and comparisons made. Results for the comparisons are described in figure 15, figure 16 and figure 18. Figure 15 observed (OBS) and simulated (WXG) rainfall are closely comparable in the year period between 1996 to 2005. From figure 15, the observed rainfall monthly time series plot has got a little bit longer amplitudes than for the simulated. A comparison between the long-term monthly means of precipitation and temperature are described in figure 16 and figure 17 respectively for the calibration period from 1996 to 2005. The observed climate samples in the period were set aside for validation of the models. The monthly temperature cycle signals were captured quite well by the monthly models with overall slight underestimation. For rainfall, however, the model appears to miss the September and October long-term seasonal climate cycles just as much as it overestimates the amounts in August

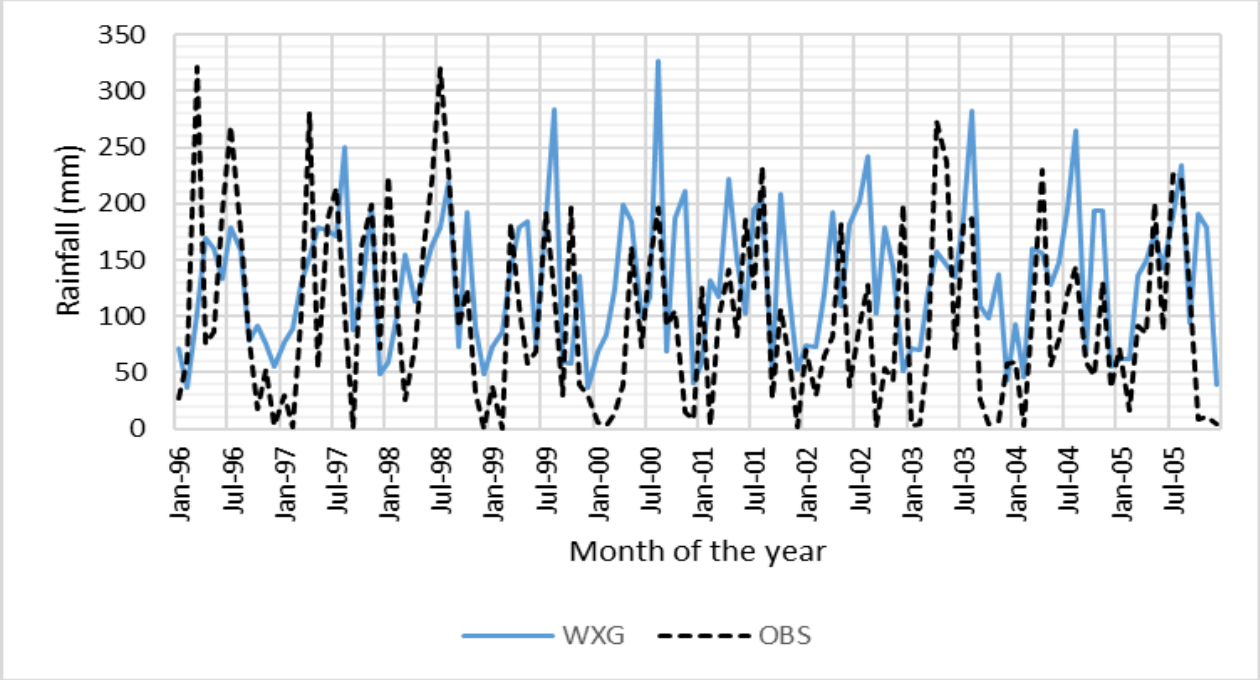

Figure 15: Mean monthly observed (OBS) and simulated rainfall (WXG) for 1996 to 2005

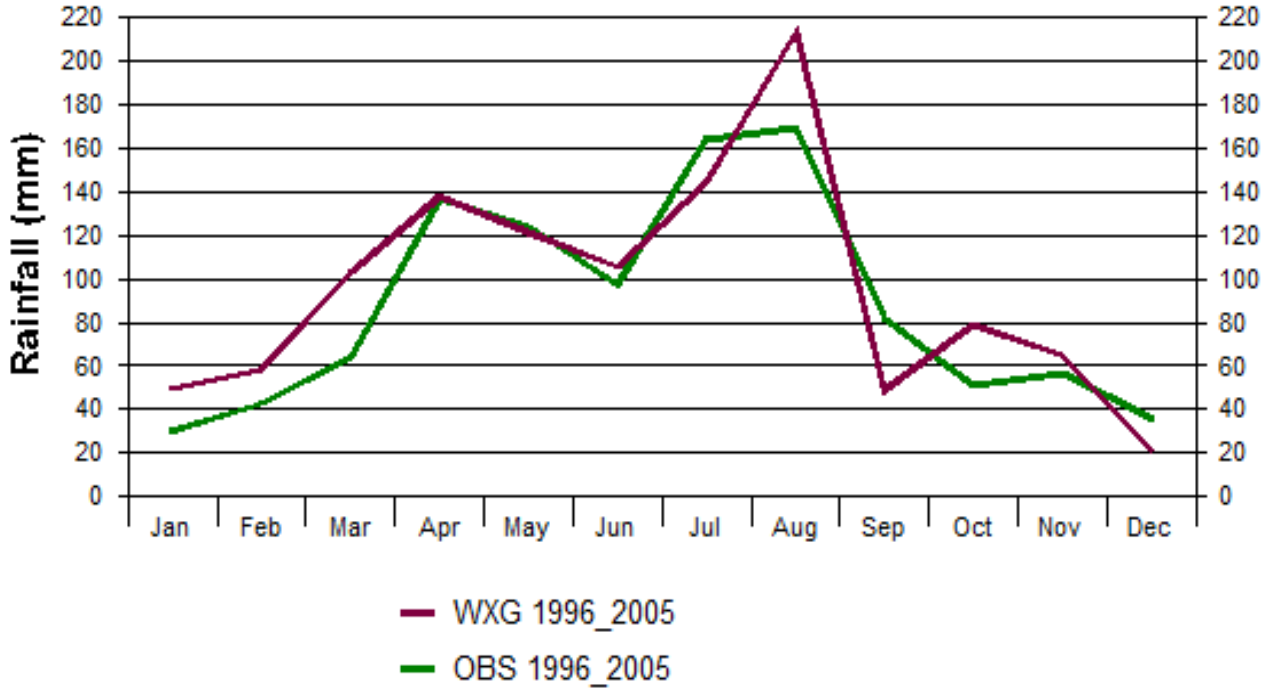

Figure 16: Monthly observed rainfall (OBS) and simulated climate (WXG) for 1996 to 2005.

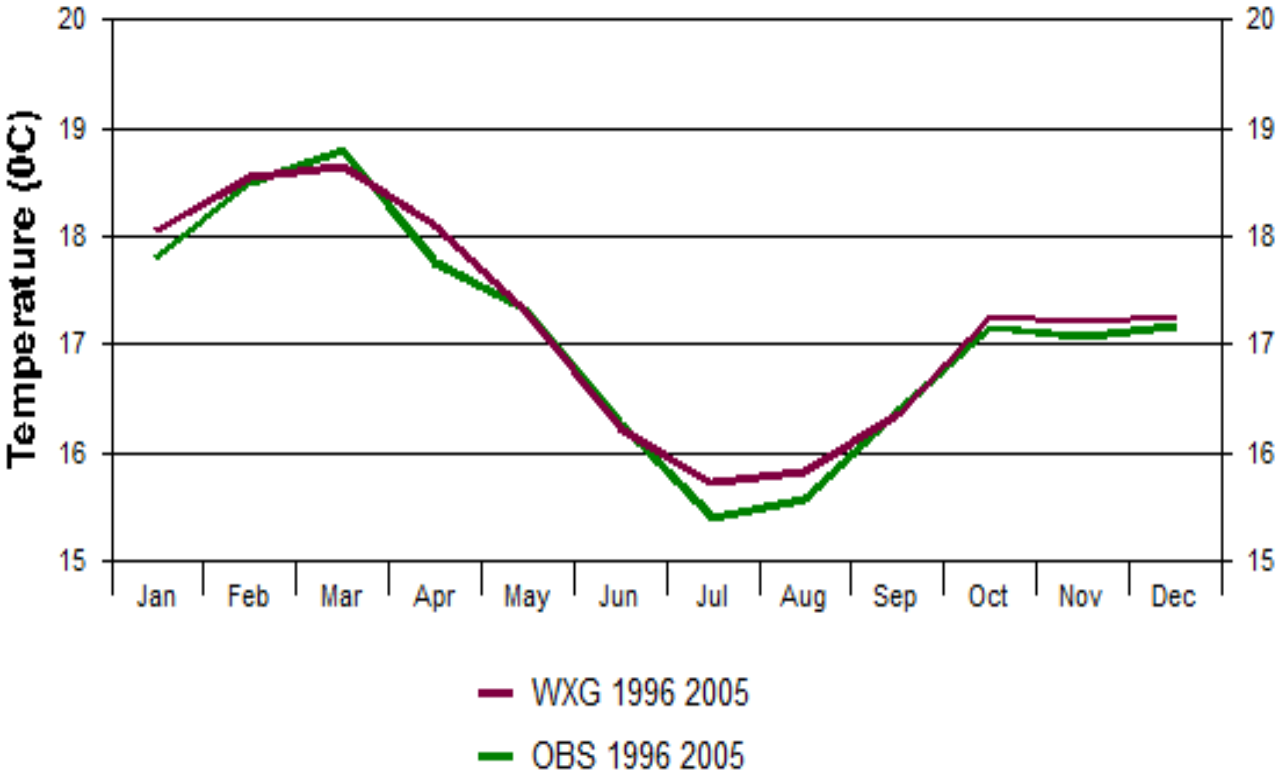

Figure 17: Monthly observed temperature (OBS) and simulated climate (WXG) for 1996 to 2005

4.5 Future climate characteristic generation and analysis

This section describes the year by year time series and trend analysis with special interest to the near-term period (2010-2039).

4.5.1 Annual time Series and Trend Analysis

Under this sub-section, we present results for downscaled daily future rainfall and temperature scenarios year by year under different representative concentration pathways (RCPs). Figure 18 depicts that monthly rainfall for the period 2010-2039 are generally higher compared to the present climate with similar seasonal signals. Figure 19 shows a combined outlook of the observed (1974-2017) and the simulated yearly rainfall characteristics under different RCP 4.5 and RCP 8.5 (2006-2099). Individual rainfall and temperature synthesized under the RCPs are shown in figures 19 to 23. The combined time series plots in figure 19 show a rising trend for the observed and a downward trend for the simulated rainfall. All the individual climate variable time series plots except figure 21 (decrease rainfall trend under RCP 8.5) do not indicate any visible trends.

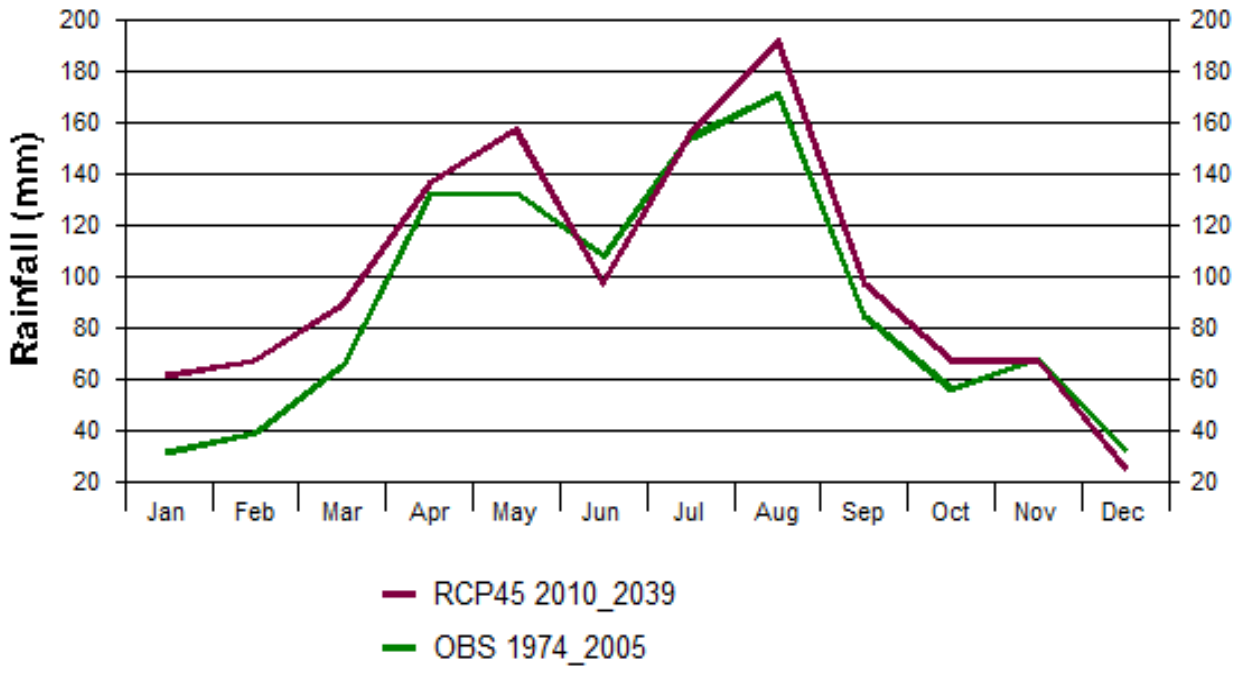

Figure 18: Monthly rainfall for present climate (1974-2005) versus simulated RCP 4.5 (2010-2039)

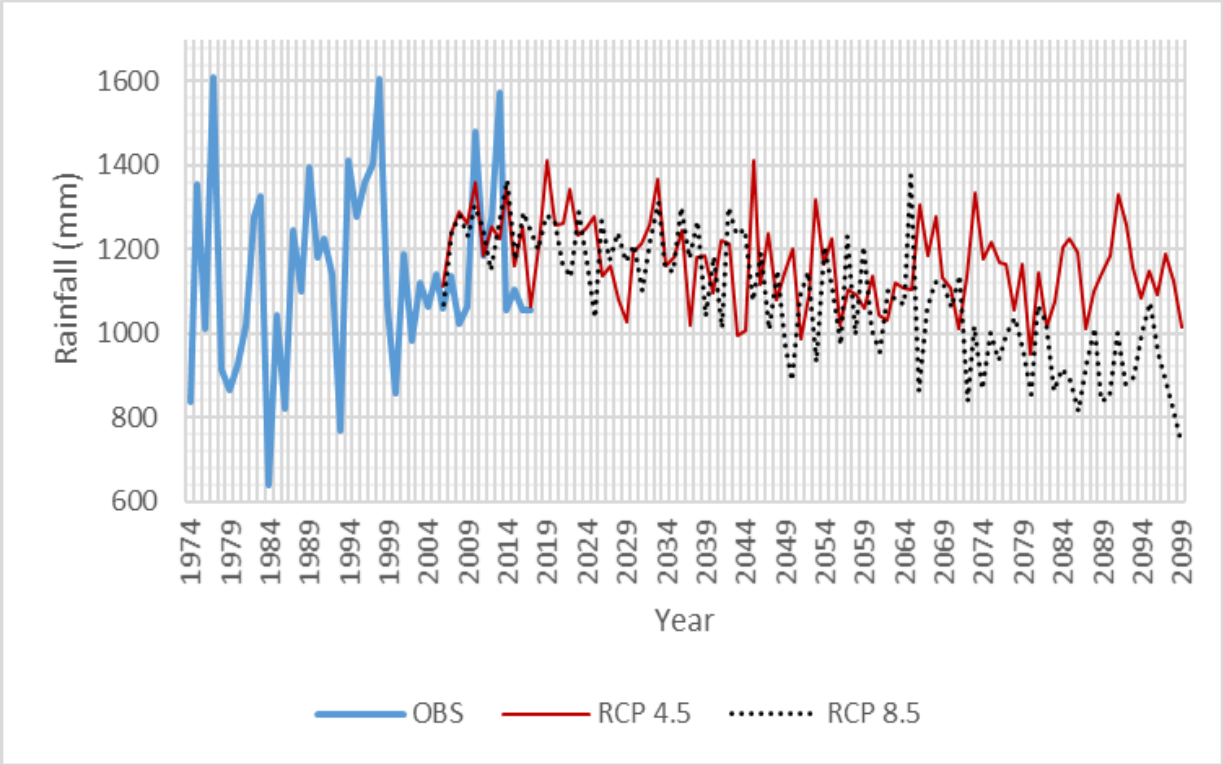

Figure 19: Annual time series for the present climate (1974-2017) and simulated rainfall (2010-2039)

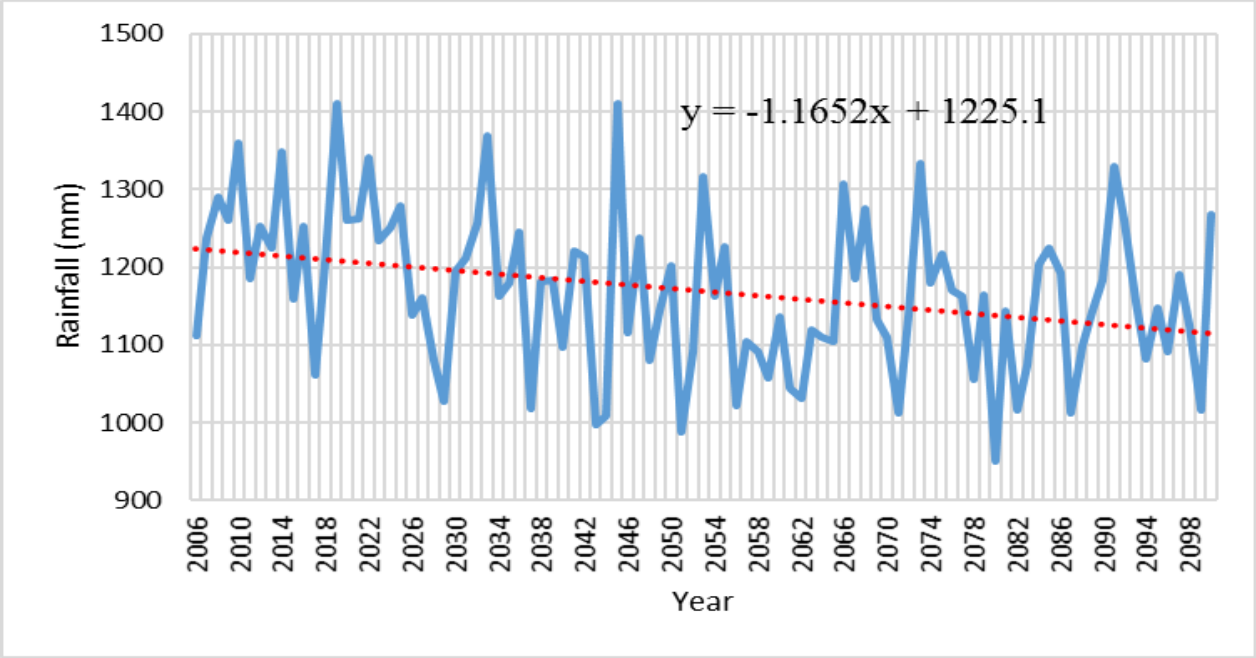

Figure 20: Time series plot for rainfall RCP 4.5 Scenario

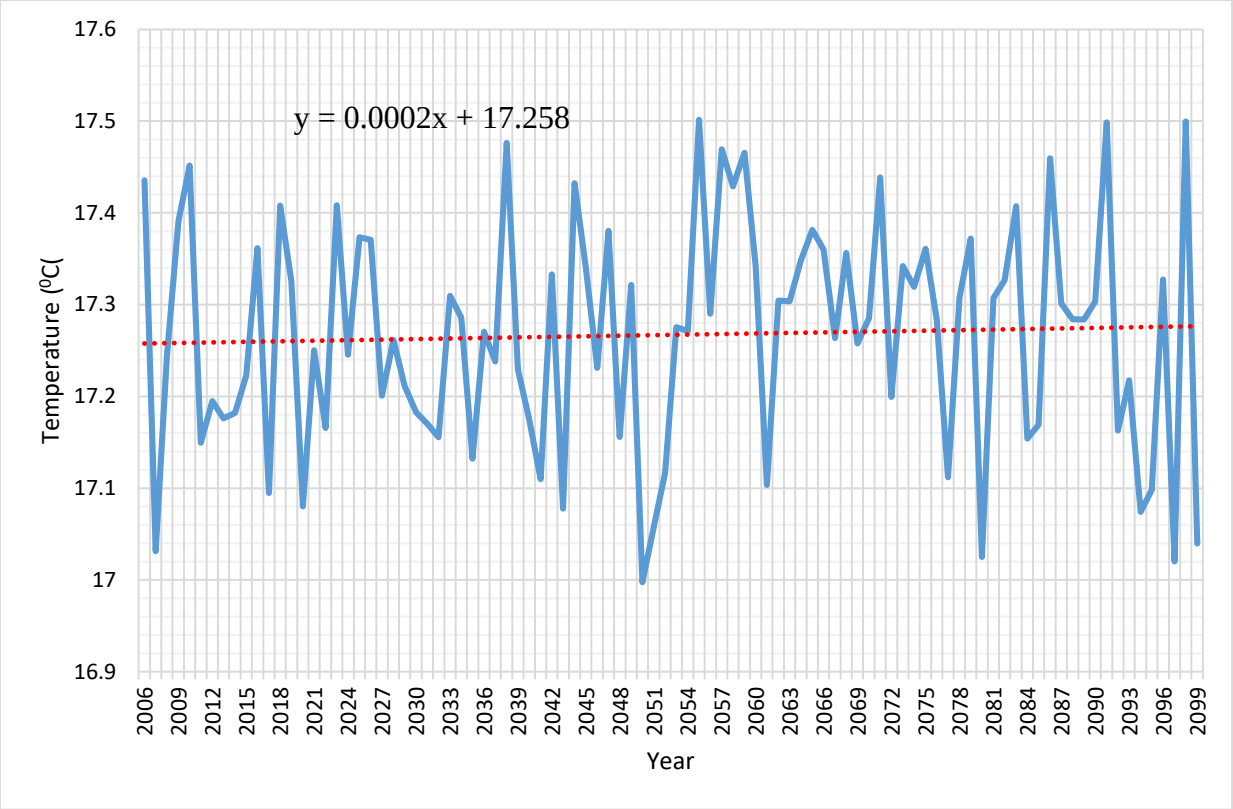

Figure 21: Time series plot for temperature (^{0}C) under RCP 4.5 Scenario

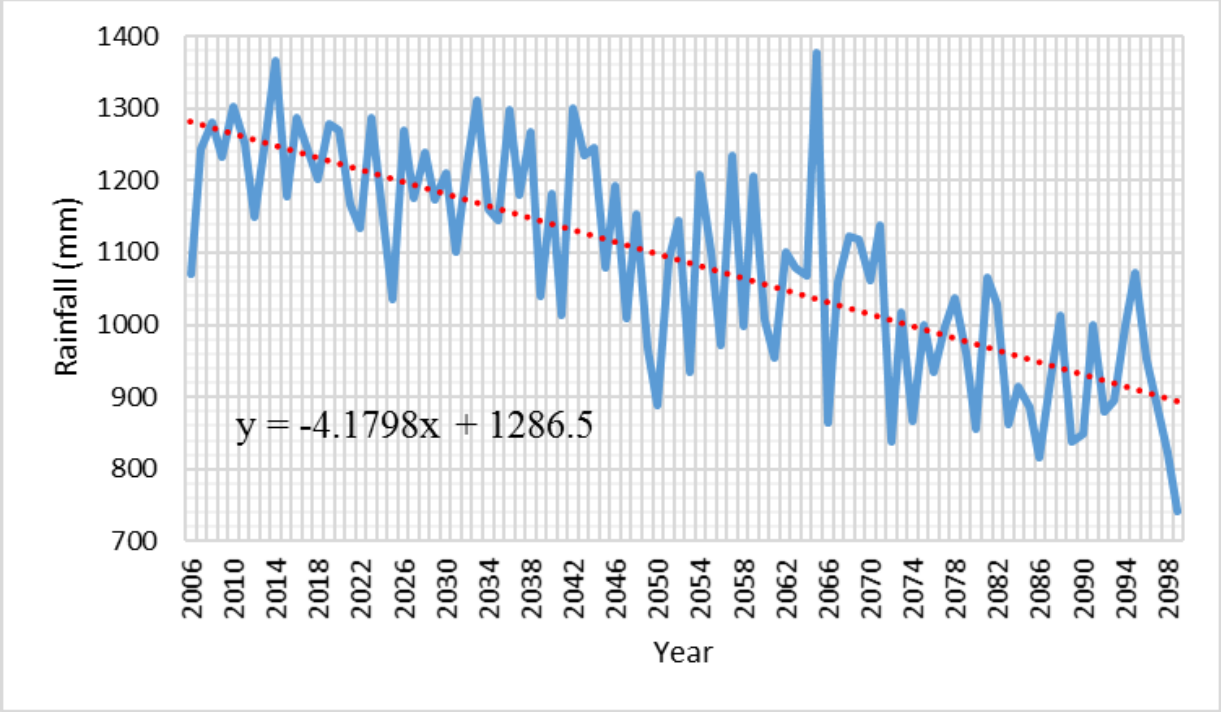

Figure 22: Time series plot for rainfall (mm) RCP 8.5 Scenario

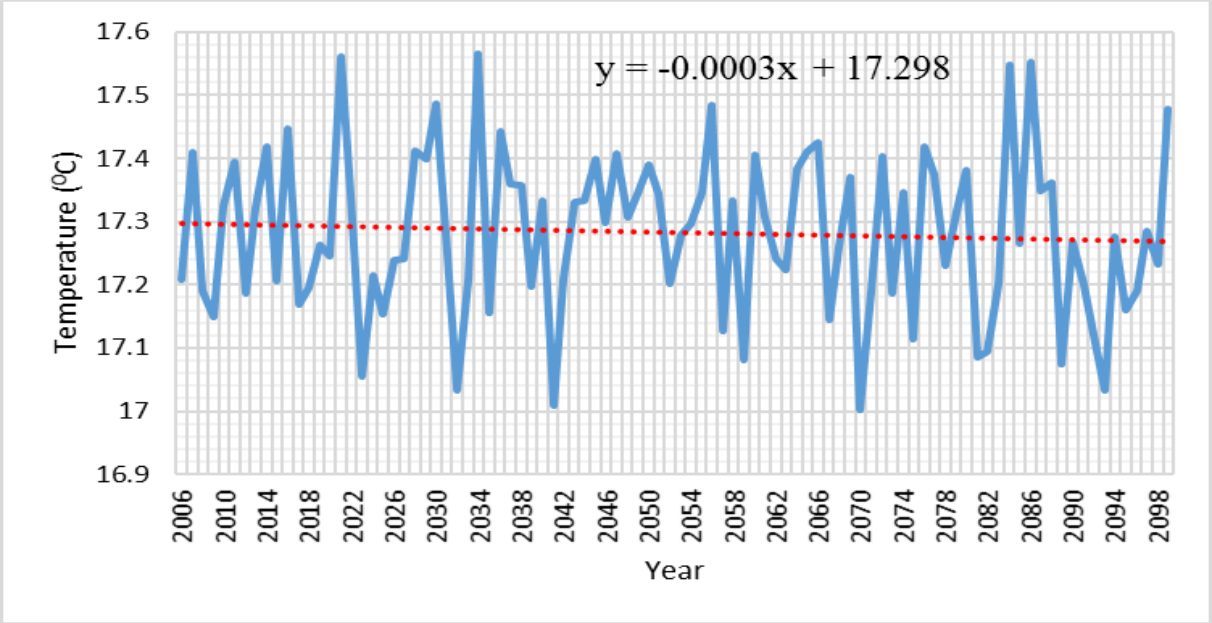

Figure 23: Time series plot for average temperature (^{0}C) RCP 8.5 Scenario

Once satisfied with the first impression of the time series plots, a Mann-Kendall statistical test was determined.

The test for the trend, at 5% significance level, was carried out using Mann-Kendall Trend test with null ($H_{0)}$ and alternative ($H_{1)}$ hypotheses as follows:

Rainfall H_0: No Trend vs. H_1: Downward Trend

Temperature H_0: No Trend vs. H_1: Upward Trend

The results obtained for RCP 4.5 and RCP 8.5 p-values (0.001 and 0) in table 19 show a notable downward trend at 5% significance level. Similarly, the slope estimates (-1.211 and -4.19) in table 20 for both scenarios indicate a negative magnitude implying a decreasing trend. From the slope estimates, the future rainfall, from 2006-2099 under RCP 4.5 and RCP 8.5, for Eldoret Meteorological Station decrease by about 1.2mm/year and 4.2 mm/year respectively. In the case of temperature, there is no significant upward trend as indicated by p-values 0.317 and 0.706 in table 19 for RCP 4.5 and RCP 8.5 respectively. To add unto this, the slope estimates in table 20

for both RCPs are of zero magnitude implying no trend over time in the simulated temperatures for the period 2006-2099.

Table 19: Mann-Kendall test statistic and p-value at 95% confidence interval

	Statistic	ASE	Z	p-Value
Rainfall RCP 4.5	-949	311.033	-3.048	0.001
Rainfall RCP 8.5	-2,445	306.16	-7.983	0
Temperature RCP 4.5	147	306.160	0.477	0.317
Temperature RCP 8.5	-167	306.160	-0.542	0.706

Table 20: Kendall Tau Statistic and the estimated slope

	Slope Estimate	95% Lower Limit	Kendall Tau Statistic
Rainfall RCP 4.5	-1.211	-0.607	-0.213
Rainfall RCP 8.5	-4.19	-3.592	-0.559
Temperature RCP 4.5	0.000	-0.001	0.034
Temperature RCP 8.5	0.000	-0.001	-0.038

4.5.2 Analysis for the predicted climate in the Near-Term (2010-2039) Period

An effort was made to compare means of the present and the near-term rainfall. Two samples of rainfall of the same sizes (40 year) were selected from the observed (2080-2009) and the near-term simulated RCPs (2010-2039). In order to do this, student-t test of hypothesis was utilized in the study. The statistical dot density, box and whisker, and density plots in figure 24 and figure 25, and the corresponding statistics summarized in table 21 and table 22 were used for the comparison. Figure 24 and figure 25 shows that the near-term rainfall under RCP 4.5 and RCP 8.5 is higher than the present climate. Table 21 shows a percentage increase of rainfall in the near-term of about 8% and 22% for the RCP 4.5 and RCP 8.5 respectively. The p-values of 0.043 and 0 in table 22 supports the alternative hypothesis that there is an increase in the near-term under the RCP 4.5 and RCP 8.5 respectively.

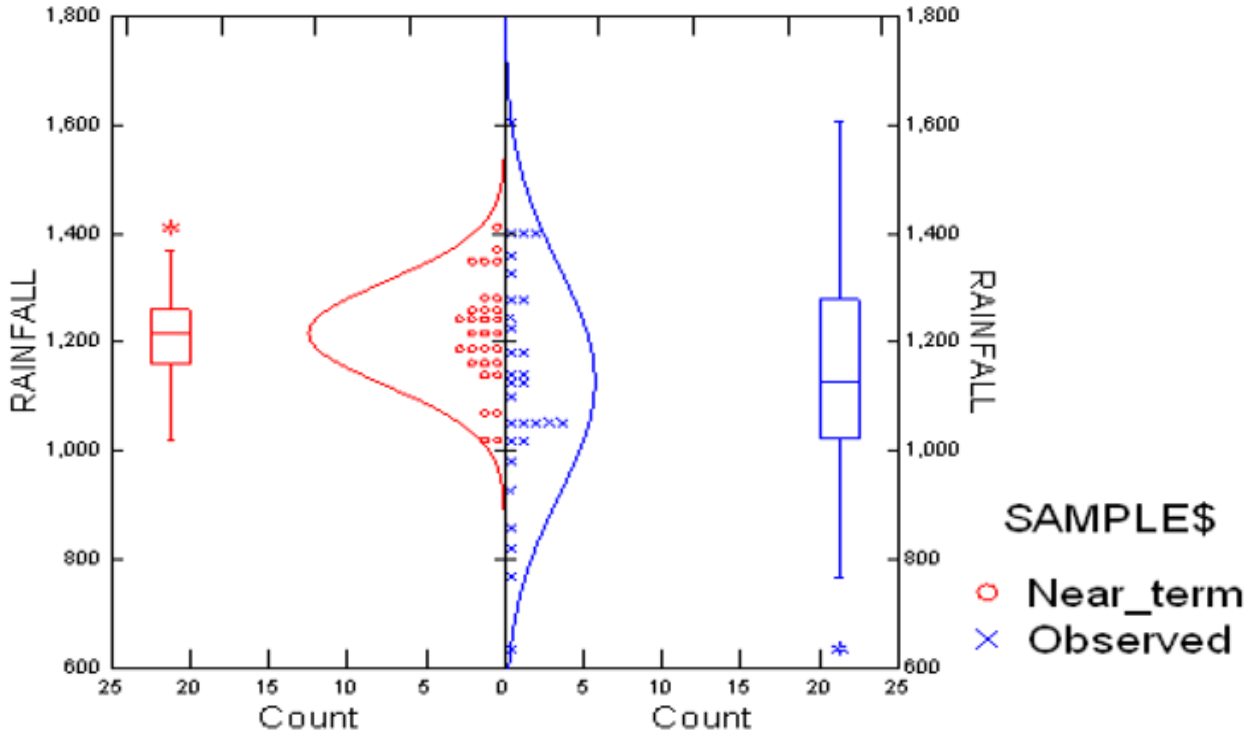

Figure 24: Dot density, box and whisker, density plots for rainfall under RCP 4.5

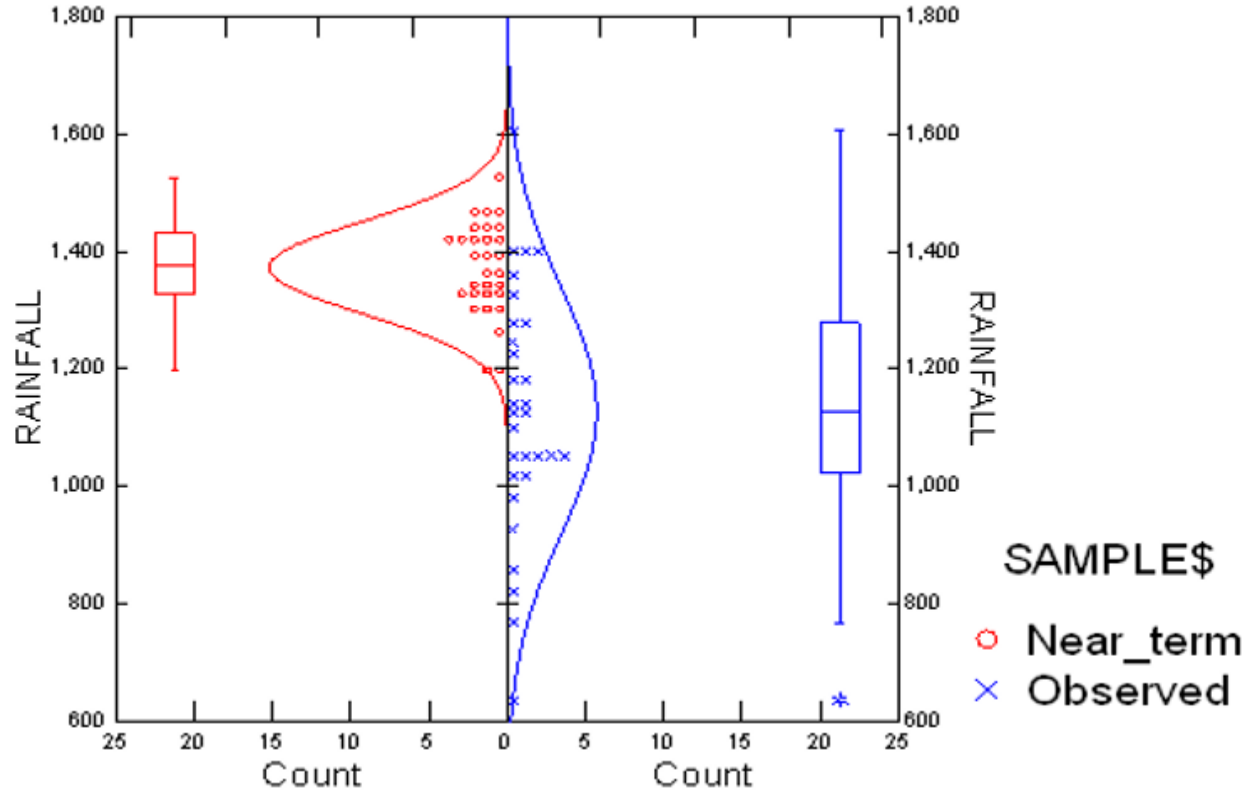

Figure 25: Dot density, box and whisker, density plots for rainfall under RCP 8.5

Table 21: Hypothesis testing of 1980-2017 and 1996-2017 rainfall inter-annual samples

Variable	Samples	N	Mean	Standard Deviation	Relative change (%)
Rainfall RCP 4.5	Near-term	30.000	1,216.352	95.924	7.793922
	Observed	30.000	1,128.405	209.180	
Rainfall RCP 8.5	Near-term	30.000	1,372.329	78.602	21.61671
	Observed	30.000	1,128.405	209.180	

Table 22: Separate variance of the 1974-1995 and 1996-2017 rainfall inter-annual samples

Variable	Sample	Mean Difference (A- B)	95% Confidence Bound (lower limit)	95% Confidence Bound (Upper limit)	t statistic	Degrees of freedom (df)	p-value
Rainfall RCP 4.5	Near-term	87.947	3.075	172.818	2.093	40.680	0.043
	Observed						
Rainfall RCP 8.5	Near-term	243.924	161.262	326.587	5.979	37.029	0.000
	Observed						

Annual and seasonal time series plots for the climate parameters (rainfall and temperature) were plotted and then trend analysis carried out. The give an indication of the trends inherent in the datasets over time, at 95% confidence interval, hypothesis test was applied. Mann-Kendall Trend test with null ($H_{0)}$ and alternative ($H_{1)}$ hypotheses used were as follows:

Rainfall H_0: No Trend vs. H_1: Downward Trend

Temperature H_0: No Trend vs. H_1: Upward Trend

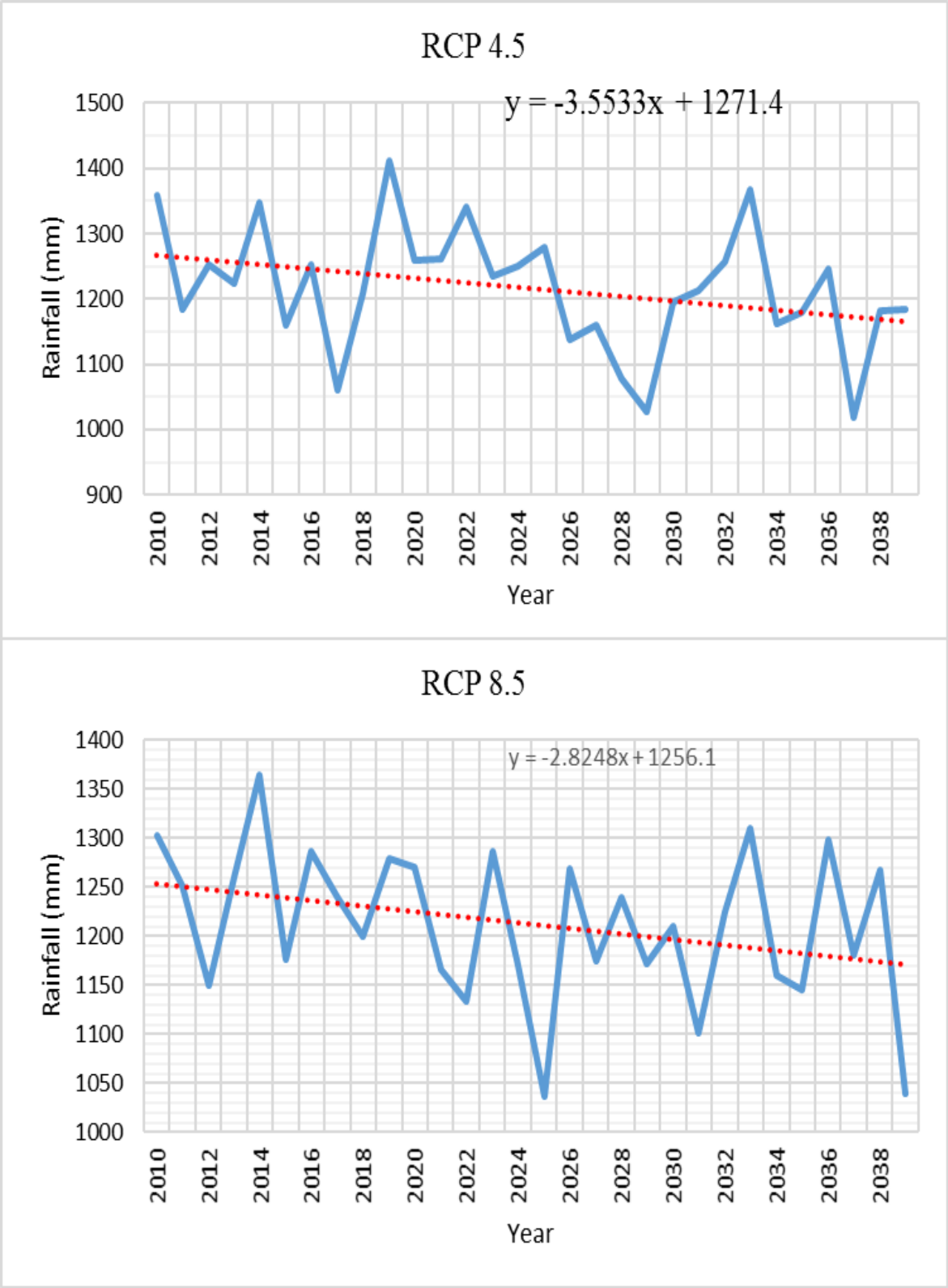

Figure 26: Rainfall RCP 4.5 and RCP 8.5 time series for near-term period (2010-2039)

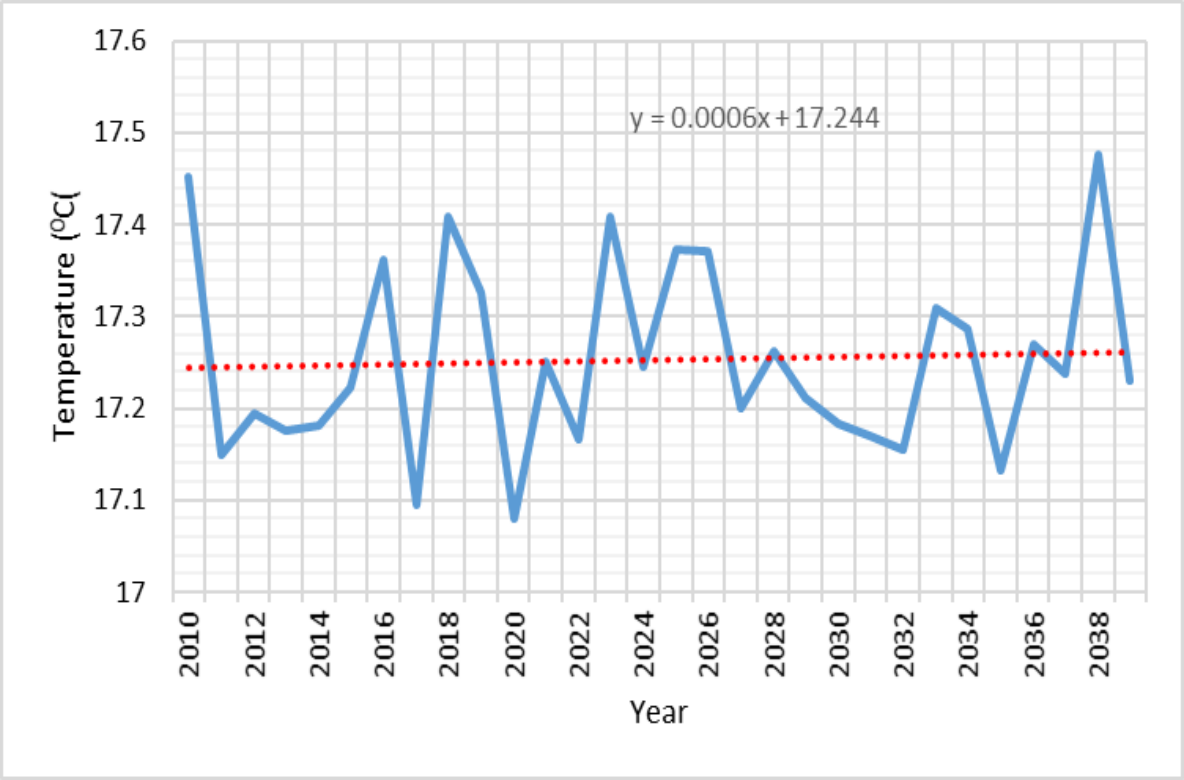

Figure 27: Temperature RCP 4.5 time series for near-term period (2010-2039)

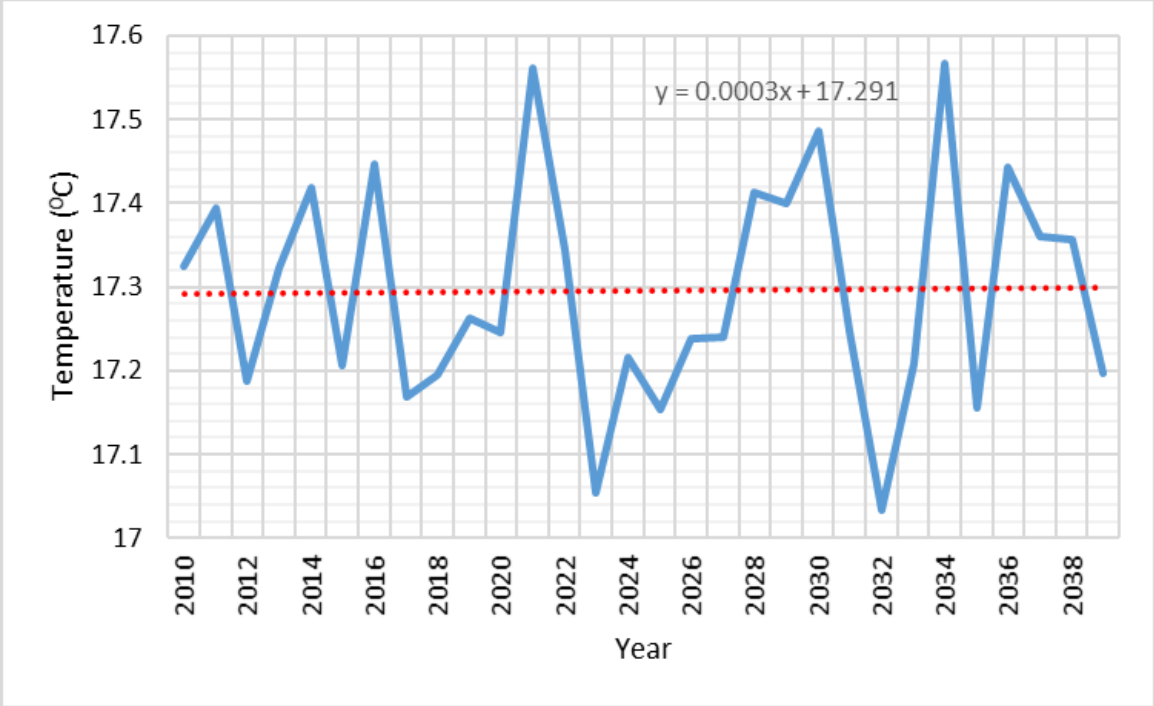

Figure 28: Temperature RCP 8.5 annual time series for near-term period (2010-2039)

Table 23: Mann-Kendall test statistic and p-value for rainfall and temperature at 95% confidence interval

Climate Parameter	Statistic	ASE	Z	p-Value
Rainfall RCP 4.5	-93	56.051	-1.641	0.950
Rainfall RCP 8.5	-87	56.051	-1.534	0.062
Temperature RCP 4.5	17	56.051	0.285	0.388
Temperature RCP 8.5	7	56.051	0.107	0.457

Table 24: Kendall Tau Statistic and the estimated slope

Climate Parameter	Slope Estimate	95% Lower Limit	Kendall Tau Statistic
Rainfall RCP 4.5	-3.069	0.050	-0.214
Rainfall RCP 8.5	-2.737	0.277	-0.200
Temperature RCP 4.5	0.001	-0.005	0.039
Temperature RCP 8.5	0.000	-0.005	0.016

Results for the p-values (0.95 and 0.062) in table 19 do not support if there is a significant downward trend for the simulated rainfall under RCP 4.5 and RCP 8.5. However, the slope estimates -3.069 and -2.737 shown in table 20 quantify the magnitude of the decreasing trend. In the case of temperature p-values (0.388 and 0.457) in table 19 do not show significant upward trend in the average temperature conditions. The slope estimates 0.001 and 0 in table 20 confirm that there is an upward trend for temperature under RCP 4.5 and no trend in RCP 8.5.

Seasonal Trend and Homogeneity Analysis was also conducted and results described by graphical plots and the corresponding statistics tabulated. Figure 29 and figure 30 shows time series plots for each of the seasons from March to May(MAM) to October to December (OND) under RCP 4.5 and RCP 8.5 respectively.

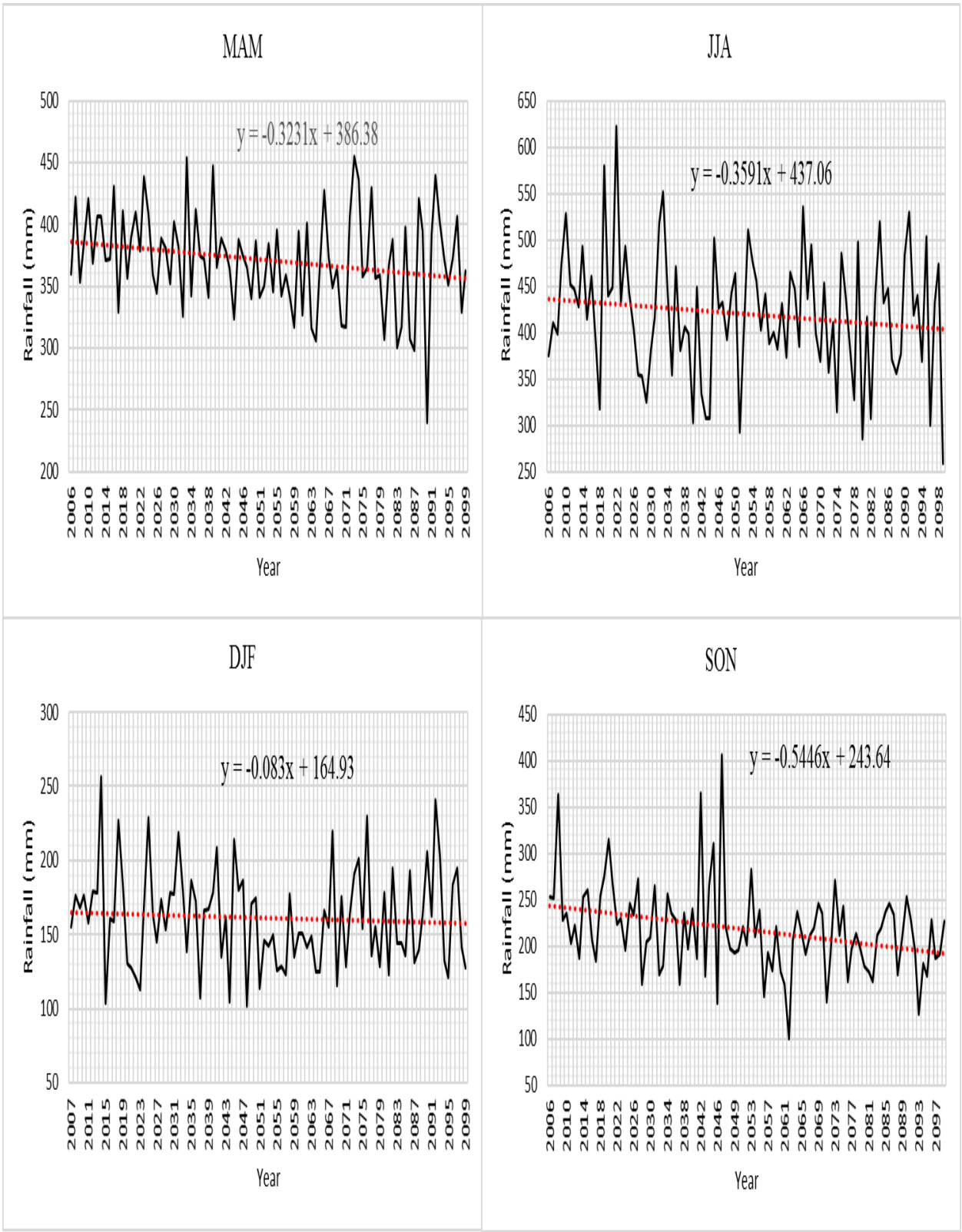

Figure 29: Seasonal rainfall Trends time series for near-term period (2010-2039) under RCP 4.5

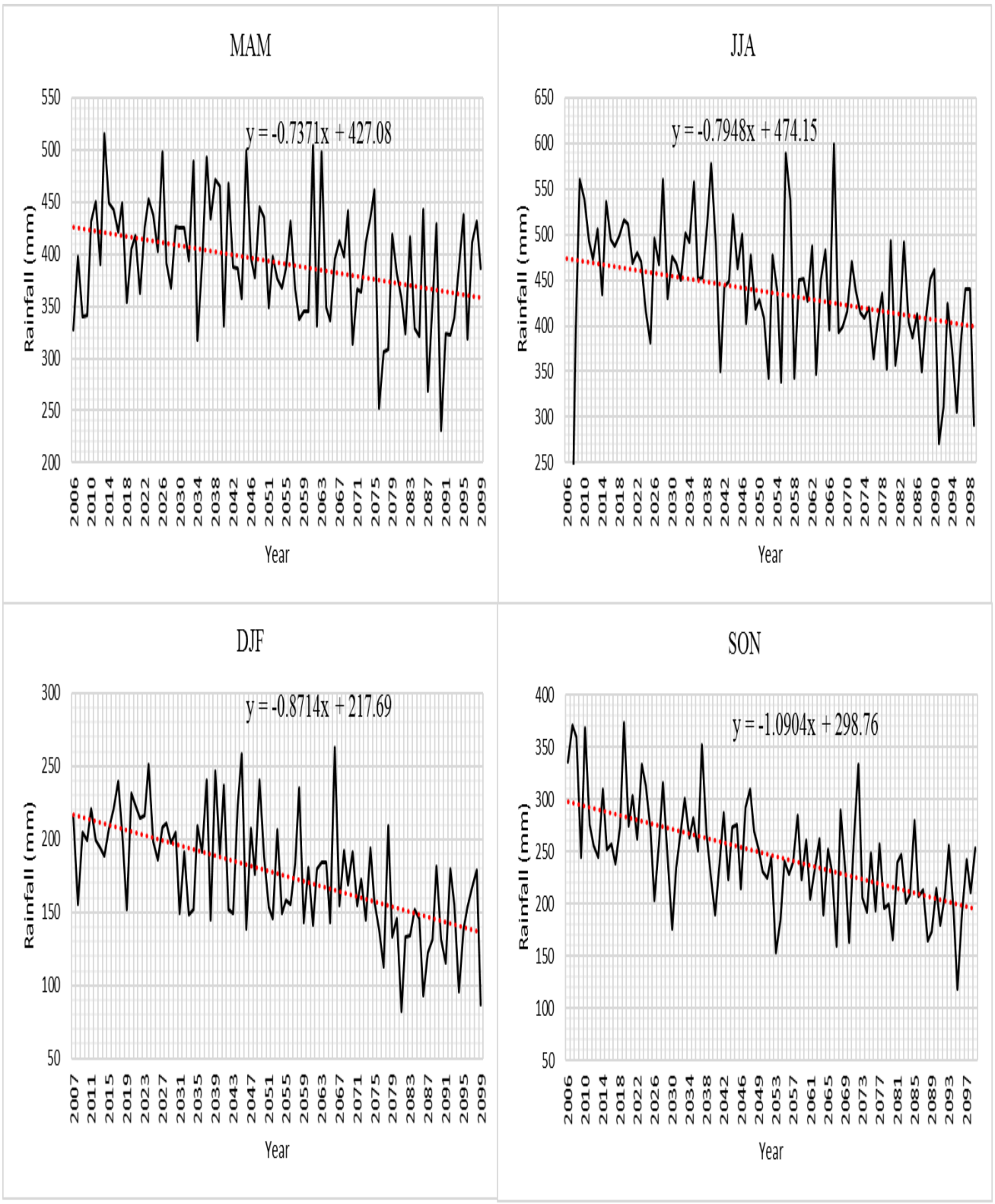

Figure 30: Seasonal rainfall Trends time series for near-term period (2010-2039) under RCP 8.5

The process of testing for trends using Mann-Kendall test in the seasons began with the formulation of the null (H_0) and alternative (H_1) hypotheses:

H_0: No Trend vs. H_1: Downward Trend

For homogeneity test the following hypotheses were used:

H0: Homogeneous Seasonal Trend vs. H1: Non Homogeneous Seasonal Trend

H0*: No Trend vs. H1*: Presence of Monotonic Trend

The computed hypothesis test results are indicated in table 25 and table 26.

Table 25: Mann-Kendall statistics for seasonal trend and homogeneity test results under RCP 4.5 and RCP 8.5

RCP	Test type	Statistic	Degrees of freedom	p-Value
RCP 4.5	Homogeneity	1.299	3	0.729
	Trend	4.258	1	0.039
RCP 8.5	Homogeneity	1.297	3	0.730
	Trend	2.164	1	0.141

Table 26: seasonal trend slope and tau statistics

RCP	Statistic	ASE	Z	p-Value	Slope Estimate	95% Upper Limit	Tau Statistic
RCP 4.5	-220.000	106.621	-2.063	0.020	-0.930	-0.139	0.135
RCP 8.5	-165.000	110.756	-1.490	0.068	-0.634	0.112	-0.096

Under RCP 4.5 results in table 25 indicate a significant (p-value=0.729) homogeneous seasonal and monotonic trend and the presence of a downward monotonic trend p-value=0.039 and slope estimate =-0.93) in general over the near-term period. In the case under RCP 8.5 results show a significant (p-value=0.73) homogeneous seasonal trend but it does not point out to a significant (p-value=0.141) presence of monotonic trend. However, in table 26, the slope gives a magnitude (-0.93 and -0.634) for RCP 4.5 and RCP 8.5 with which the seasons experience a downward monotonic trend in general.

CHAPTER FIVE

5.0 Conclusions and Recommendations

In this section conclusions and recommendation from the findings of the project study are discussed.

5.1 Conclusions

The observed rainfall for Eldoret Meteorological Station from 1974 to 2017 show a significant percentage increase of approximately 5.6 % between the sampled periods (1974-1995 and 1996-2017). Analysis of trend technique also proved that rainfall has been increasing in the present climate. However, the simulated rainfall under RCP 4.5 and RCP 8.5 indicate a downward trend both in the near-term (2010-2039) and in the overall (2006-2099) time periods.

In the predictor screening stage, selection of the most appropriate predictors is a difficult task. Any chosen predictor dictates the kind of downscaled scenarios of climate. Once chosen for model calibration, predictors are used month by month throughout the simulation period. It is not always the case that variabilities of the predictors remain the same, as is the assumption, but do exhibit spatio-temporal changes over time.

The results for the future downscaled rainfall for Eldoret Meteorological Station indicate a significant decrease for both RCP 4.5 and RCP 8.5 scenarios. Under RCP 4.5, it is expected that the rainfall will follow a downward trend with a rate of approximately 12 mm/decade from 2006-2099. For the same period, RCP 8.5 scenarios for the station will decrease at the rate of about 42 mm/decade. The findings of this study show that for the period 1974-2017, the observed average temperature indicate that there has been a warming of 0.08 0C/decade in the current climate.

Results for this study show that Eldoret Meteorological Station and its neighborhood is expected to experience warming in the near-term period under RCP4.5 at the rate of 0.01^0C per decade. The findings of the study anticipate a general drying over time over time under the both RCPs for both near term and overall period.

Although the model has indicated a decrease in rainfall over time, there is a possibility of increased frequencies of above normal rainfall which will result in flooding. Eldoret town, has recently experienced rapid development hence increase concrete surface. What this means, in an event of above normal rainfall, is just but flooding. Road, building and construction sectors need to consider redesigning bridges, water ways and related structures to help curb the predicted floodings menace.

The outcome of the study will provide information about the future climate characteristics that can be used to inform policymaking. Information about the finer temporal and spatial details projected daily Rainfall and temperature is applicable for use in impact assessment, agricultural and hydrological studies. It can be used to prepare in advance for mitigation and adaptation strategies by enacting appropriate legislation to the changing climate.

5.2 Recommendations

In the study, we have dealt with the present and the possible future climate conditions and trends at Eldoret Meteorological Station. There is a need to extend this research to find out the possible economic, social and environmental impacts corresponding to such changes and trends in the monthly, seasonal and inter-annual trends and variabilities. We acknowledge a substantial amount of missing daily data which we estimated using the monthly means. We recommend the future similar research should strive to find a way to use a more complete and possibly augment with remote sensed datasets from satellites for finer details.

The results from the projected near-term period projected climatology indicate a significant warming and a significant downward trend of rainfall. It is incumbent upon the policy makers and all the stakeholders, especially in the agricultural industry to attempt to put up strategies to adapt to the changing climate, including possible changes in the policy agenda.

Over the study area, we advise farmers and the policy makers in the agricultural sector to find ways of diversifying livelihoods other than engaging in maize and wheat alone. The slowly diminishing rainfall requires the growing of drought resistant crop varieties in Uasin-Gishu County and its neighborhoods. As has been shown through research, the warming of the study area will

possibility lead to insurgence of the vectors such as malaria causing mosquitoes, commonly known as highland malaria, hence the health sector ought to plan well in advance.

As will be permitted by the data availability, a similar study for the neighbouring stations need to be undertaken to validate the findings of this study. GIS and remote sensing and technology can have applied to integrate several stations in a similar study will greatly enhance the usability and practicality of the study results. It will also be very important to carry out impact assessment associated with the results of this research study.

CHAPTER SIX

6.0 References

Arora, V. K., Boer, G. J., Christian, J. R., Curry, C. L., Denman, K. L., Zahariev, K., … Lee, W. G. (2009). The Effect of terrestrial photosynthesis down regulation on the twentieth-century carbon budget simulated with the CCCma Earth System Model. *Journal of Climate*, *22*(22), 6066–6088. https://doi.org/10.1175/2009JCLI3037.1

Brekke, L., Thrasher, B. L., Maurer, E. P., & Pruitt, T. Downscaled CMIP3 and CMIP5 Climate Projections (2013). Retrieved from http://gdo-dcp.ucllnl.org/downscaled_cmip_projections/

Daksiya, V., Mandapaka, P., & Lo, E. Y. M. (2017). A Comparative Frequency Analysis of Maximum Daily Rainfall for a SE Asian Region under Current and Future Climate Conditions. *Hindawi Advances in Meteorology*, *2017*. https://doi.org/10.1155/2017/2620798

Feyissa, G., Zeleke, G., Bewket, W., & Gebremariam, E. (2018). Downscaling of Future Temperature and Precipitation Extremes in Addis Ababa under Climate Change. *Climate*, *6*(58). https://doi.org/10.3390/cli6030058

Huho, J. M., & Mugalavai, E. (2010). The Effects of Droughts on Food Security in Kenya. *The International Journal of Climate Change*, *2*(January). https://doi.org/10.18848/1835-7156/CGP/v02i02/37312

Ininda, J. M., Athumani, C., & Mutemi, J. N. (2008). Towards improvement of seasonal rainfall forecasting through model output statistics (MOS) downscaling of Echam forecasts over Tanzania. *Journal of the Kenya Meteorological Society*, *2*(1–2), 99–108.

IPCC. (2014). *Climate Change 2014. Synthesis Report. Contribution of Working Groups I, II and III to the Fifth Assessment Report of the Intergovernmental Panel on Climate Change [Core Writing Team, R.K. Pachauri and L.A. Meyer (eds.)]*. IPCC, Geneva, Switzerland. https://doi.org/10.1016/S0022-0248(00)00575-3

Jones, P. G., Thornton, P. K., & Jens, H. (2009). *Generating characteristic daily weather data using downscaled climate model data from the IPCC's Fourth Assessment*.

Keellings, D. (2016). Short Communication Evaluation of downscaled CMIP5 model skill in simulating daily maximum temperature over the southeastern United States. *International Journal of Climatology*, (October 2016). https://doi.org/10.1002/joc.4612

Koukidis, E. N., & Berg, A. A. (2010). Sensitivity of the Statistical DownScaling Model (SDSM) to reanalysis products Sensitivity of the Statistical DownScaling Model (SDSM) to Reanalysis Products, *5900*. https://doi.org/10.3137/AO924.2009

Meehl, G. A., Stocker, T. F., Collins, W. D., Friedlingstein, P., Gaye, A. T., Gregory, J. M., … Zhao, Z.-C. (2007). Global Climate Projections. In: Climate Change 2007. In *The Physical Science Basis. Contribution of Working Group I to the Fourth Assessment Report of the Intergovernmental Panel on Climate Change [Solomon, S., D. Qin, M. Manning, Z. Chen, M. Marquis, K.B. Averyt, M. Tignor and H.L. Miller (eds.)]* (pp. 748–845). Cambridge, United Kingdom and New York, NY, USA: Cambridge University Press. https://doi.org/10.1109/ICEPT.2010.5582830

Mtongori, H. I., Stordal, F., & Benestad, R. E. (2016). Evaluation of Empirical Statistical Downscaling Models ' Skill in Predicting Tanzanian Rainfall and Their Application in Providing Future Downscaled Scenarios. *American Meteorological Society, 29*, 3231–3252. https://doi.org/10.1175/JCLI-D-15-0061.1

Muraya, B. W., & Ruigu, G. (2017). Determinants of Agricultural Productivity in Kenya, *V*(4).

Myhre, G. D., Shindell, F. M., Bréon, W., Collins, J., Fuglestvedt, J., Huang, D., … Zhan, H. (2013). Anthropogenic and Natural Radiative Forcing. In *Climate Change 2013: The Physical Science Basis: Working Group I Contribution to the Fifth Assessment Report of the Intergovernmental Panel on Climate Change [Stocker, T.F., D. Qin, G.-K. Plattner, M. Tignor, S.K. Allen, J. Boschung, A. Nauels, Y. Xia, V.* (Vol. 9781107057, pp. 659–740). Cambridge, United Kingdom and New York, NY, USA.: Cambridge University Press. https://doi.org/10.1017/CBO9781107415324.018

Okkan, U., & Kirdemir, U. (2016). Downscaling of monthly precipitation using CMIP5 climate models operated under RCPs. *Royal Meteorological Society, 528*, 514–528. https://doi.org/10.1002/met.1575

Rwigi, S. K., Muthama, J. N., Opere, A., Opijah, F. J., & Gichuki, F. N. (2016). Simulated Impacts of Climate Change on Surface Water Yields over the Sondu Basin in Kenya.

Sonwa, D. J., Dieye, A., Mzouri, E. El, Majule, A., Mugabe, T., Omolo, N., … Brooks, N. (2016). Drivers of climate risk in African agriculture, *5529*(May). https://doi.org/10.1080/17565529.2016.1167659

Souvignet, M., Gaese, H., Ribbe, L., Kretschmer, N., Souvignet, M., Gaese, H., … Oyarzún, R. (2010). Statistical downscaling of precipitation and temperature in north - central Chile : an assessment of possible climate change impacts in an arid Andean watershed, *6667*. https://doi.org/10.1080/02626660903526045

Tahir, T., Hashim, A. M., & Yusof, K. W. (2018). Statistical downscaling of rainfall under transitional climate in Limbang River Basin by using SDSM. In *IOP Conference Series: Earth and Environmental Science 140 (2018) 012037*. https://doi.org/10.1088/1755-1315/140/1/012037

Taylor, K. E., Stouffer, R. J., & Meehl, G. A. (2012). An overview of CMIP5 and the experiment design. *Bulletin of the American Meteorological Society*. https://doi.org/10.1175/BAMS-D-11-00094.1

Thomson, A. M., Calvin, K. V, Smith, S. J., Kyle, G. P., Volke, A., Patel, P., … Edmonds, J. A. (2011). RCP 4.5: a pathway for stabilization of radiative forcing by 2100, 77–94. https://doi.org/10.1007/s10584-011-0151-4

Wilby, R. L. (2002). sdsm — a decision support tool for the assessment of regional climate change impacts. *Elsevier*, *17*, 147–159.

Wilby, R. L., & Dawson, C. W. (2004). Using SDSM Version 3 . 1 — A decision support tool for the assessment of regional climate change impacts User Manual, 1–67.

Yang, D., & Saenko, O. A. (2012). Ocean heat transport and its projected change in CanESM2. *Journal of Climate*, *25*(23), 8148–8163. https://doi.org/10.1175/JCLI-D-11-00715.1